MATERIALS CHEMISTRY
FRONTIERS

REVIEW

View Article Online
View Journal | View Issue

Cite this: *Mater. Chem. Front.*, 2021, **5**, 4424

Versatile graphene oxide nanosheets *via* covalent functionalization and their applications

Minju Park, †[a] Namhee Kim, †[a] Jiyoung Lee, †[a] Minsu Gu *[b] and Byeong-Su Kim *[a]

Received 13th January 2021,
Accepted 29th March 2021

DOI: 10.1039/d1qm00066g

rsc.li/frontiers-materials

Even though many graphene derivatives that are atomically thin two-dimensional structures, such as graphene oxide (GO), have triggered enormous interest in the scientific and industrial communities owing to their easy synthesis and mass production, there is inevitable degradation of their properties compared to pristine graphene. This is because the sp^2-carbon lattice of chemically oxidized GO is transformed into sp^3-defect sites with various oxygen-containing functional groups. However, from a synthetic chemistry perspective, GO can become a robust and versatile carbon scaffold with utilizable surface functional groups *via* a variety of synthetic methods. In this regard, covalent functionalization with a diverse set of molecules on the surface of GO can not only recover diminished electrical and physical properties but also improve its overall performance in applications. In this review, we focus on the covalent functionalization of GO and present various strategies to control its dispersibility, conductivity, and catalytic activity toward potential applications. We anticipate that graphene chemistry will offer opportunities for designing multifunctional nanocomposites for future development in the materials science and device engineering areas.

1. Introduction

Sustainability is becoming the most important aspect when developing new materials and applications. Carbon-based materials are considered paradigmatic examples of sustainability due to their high surface area, scalable production, tunable surface chemistry, and environmentally benign properties. In this regard, carbon-based materials have remained at the forefront of many fields from nanotechnology to devices and

[a] *Department of Chemistry, Yonsei University, 50 Yonsei-ro, Seoul 03722, Republic of Korea. E-mail: bskim19@yonsei.ac.kr*
[b] *Department of Chemical Engineering (BK21 FOUR), Dong-A University, Busan 49315, Republic of Korea. E-mail: sbgms@dau.ac.kr*
† These authors contributed equally to this work.

Minju Park

Minju Park received her BS from the Department of Chemical Engineering at Ulsan National Institute of Science and Technology (UNIST), Republic of Korea, in 2014 and her PhD from the Department of Chemical Engineering at UNIST in 2020 under the supervision of Prof. Byeong-Su Kim. She is currently a postdoctoral researcher in Dr Heesuk Kim's group at Korea Institute of Science and Technology (KIST). Her research interests include carbon-based nanomaterials and polymers for energy related applications.

Namhee Kim

Namhee Kim is currently an MS/PhD student in Prof. Byeong-Su Kim's group in the Department of Chemistry at Yonsei University. She received her BS from the Department of Chemistry at Chungnam National University, Republic of Korea, in 2020. Her research interests include nanomaterials and polymers for energy conversion.

are receiving increasing attention as part of the imminent 'Carbon Age'.[1–4]

Among the allotropes of the mother element, such as graphite, diamond, and fullerenes, much interest has been focused on carbon nanotubes and graphene with anisotropic one- and two-dimensional structures, respectively, with sp^2-conjugated carbon atoms densely packed in a honeycomb crystal lattice.[5,6] These unique chemical structures provide a broad spectrum of outstanding properties, such as extremely high mechanical strength, high thermal conductivity, high stability, and rich electronic properties.[7,8]

To utilize carbon nanomaterials more efficiently, non-covalent functionalization has been widely exploited,[9] based on the van der Waals forces[10–12] and π–π interactions[13–15] with organic molecules or polymers. Because of this relative weak non-covalent interaction, non-covalently functionalized carbon nanomaterials often suffer from poor dispersibility in common organic solvents and other materials, which poses critical challenges for practical applications.[16,17] On the other hand, covalent modification can offer a robust approach toward the preparation of GO derivatives with desired applications. To address these issues, a covalent chemistry approach can be employed to modify the surfaces of carbon nanomaterials for the reliable synthesis of carbon derivatives.[18,19] Furthermore, covalent functionalization of carbon nanomaterials can offer a powerful means to tailor the physical and chemical properties, providing them more practical opportunities for diverse applications. In this context, graphene oxide (GO) is an attractive alternative to pristine graphene due to its diverse functionalities, which can potentially provide great opportunity for further modifications. GO nanosheet with various reactive functional groups such as carboxylic acid, epoxide, or hydroxyl groups are prerequisites, which are generated by oxidation of graphite with strong oxidants and subsequent exfoliation of the resulting graphite oxide.[20–23] In 1859, Brodie first synthesized GO by adding potassium chlorate to graphite with fuming nitric acid.[24] After that, Hummers' method has commonly used in the synthesis of GO with potassium permanganate and sodium nitrate in concentrated sulfuric acid.[20] The most widely accepted model for GO is based on Lerf and Klinowski's model, which contains an sp^2-hybridized carbon region and oxygen-containing functional groups on the surface.[25]

The high degree of functionalization of GO *via* its multitude of epoxide, hydroxyl, and carboxylic acid groups makes it suitable for further derivatization.[22,26] In particular, significant efforts have been focused on the covalent functionalization of GO *via* exploiting classical organic transformations to tune the material's physicochemical properties, comparing to modification of chemically inert graphene.[19,27] Unlike non-covalent functionalization, covalent chemistry can offer a more robust approach toward the preparation of GO derivatives with the desired molecules to tailor the properties of pristine GO for target applications. Moreover, the electrical properties and sp^2 lattice of GO could be partially recovered through either the

Jiyoung Lee

Jiyoung Lee is currently a PhD student in Prof. Byeong-Su Kim's group in the Department of Chemistry at Yonsei University. She received her BS and MS from the Department of Chemistry at Soongsil University, Republic of Korea, in 2018 and 2020 under the supervision of Prof. Ik-Soo Shin. Her research interests include nanomaterials and polymers for energy conversion.

Minsu Gu

Minsu Gu is an Assistant Professor in the Department of Chemical Engineering at Dong-A University, Republic of Korea. He received his BS from the School of Nano-Bioscience and Chemical Engineering at Ulsan National Institute of Science and Technology (UNIST), Republic of Korea, in 2013, and his PhD from the Department of Energy Engineering at UNIST in 2018 under the supervision of Prof. Byeong-Su Kim. He was a postdoctoral researcher in Dr Allen J. Bard's group in the Department of Chemistry at the University of Texas at Austin. His research interests include the electrochemistry of functional nanomaterials and polymers for energy conversion and storage applications.

Byeong-Su Kim

Byeong-Su Kim is a Professor in the Department of Chemistry at Yonsei University, Republic of Korea. He received his BS and MS in Chemistry at Seoul National University and his PhD in Chemistry at the University of Minnesota, Twin Cities, in 2007. After his postdoctoral research at MIT, he started his independent career at UNIST in 2009 and recently moved to Yonsei University in 2018. His group investigated a broad range of topics in macromolecular chemistry for the study of novel polymer and hybrid nanomaterials, including the molecular design and synthesis of self-assembled polymers and carbon-based nanostructures.

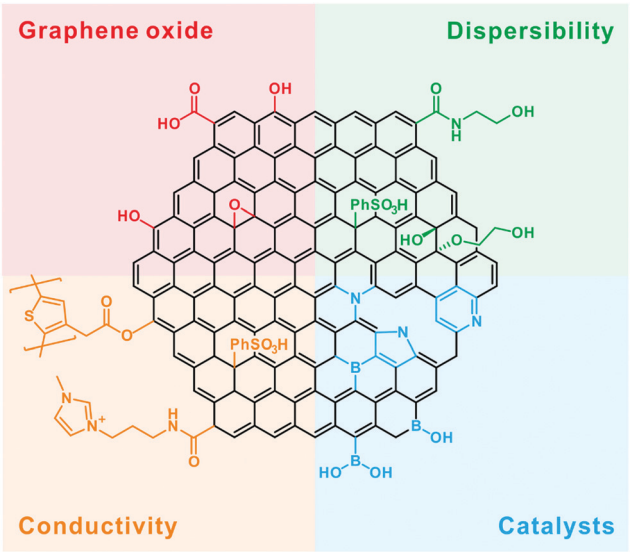

Fig. 1 A schematic representation of the utilization of GO derivatives prepared by covalent functionalization.

thermal treatments or chemical reduction. Specifically, thermal annealing under reductive environments and chemical reduction with strong reducing agents such as hydrazine,[28,29] metal hydrides,[30] and HI[31] are widely employed to provide a promising alternative toward the large-scale synthesis of GO nanosheets with improved electrical properties.[32,33]

While the properties and application of GO have been extensively reviewed so far, in this review, we aim to cover the recent progress in the covalent functionalization of GO and its subsequent applications (Fig. 1). Specifically, we address how chemical modification can tune the properties of GO, such as dispersibility, electrical and thermal conductivity, and catalytic activity, toward realizing the desired application.

2. Covalent functionalization

Functionalization of GO is categorized into two parts: edge-group and basal-plane modification of GO nanosheets (Fig. 2).

2.1 Edge-group modification

In most approaches, carboxylic acid groups are transformed into active sites and used for conversion into esters or amides (Fig. 2b). In general, carboxylic acid groups on GO nanosheets can be activated by using thionyl chloride ($SOCl_2$) to produce the reactive intermediate, acyl chloride, for further condensation reactions.[34–36] Furthermore, the carboxylic acid group can be activated by coupling agents such as 1-ethyl-3-(3-dimethylaminopropyl)carbodiimide (EDC),[37–39] or *N*,*N*′-dicyclohexylcarbodiimide (DCC),[40] followed by condensation with nucleophilic alcohols or amines, typically in excess, to proceed the reaction. In carbodiimide coupling chemistry, GO is exfoliated in a polar solvent (typically *N*,*N*′-dimethylformamide (DMF), 1-methyl-2-pyrrolidinone (NMP), or water) and then treated with an activator such as 4-dimethylaminopyridine (DMAP) or *N*-hydroxysuccinimide (NHS).

As a representative example, our group has widely employed EDC chemistry for the modification of carboxylic acid groups.[39,41–45] For example, the carboxylic acids in GO can be replaced with amine groups through the formation of amides using various amines such as ethylenediamine and ethanolamine. Furthermore, a multitude of macromolecules can be employed for the edge functionalization of GO nanosheet, including chitosan,

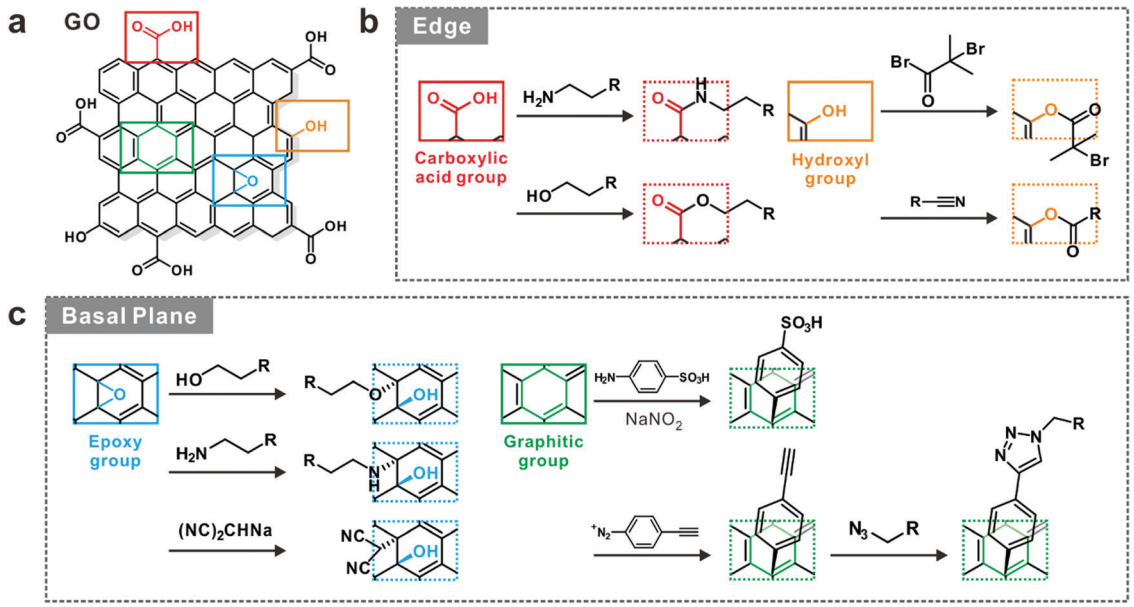

Fig. 2 Representative types of reactions for the functionalization of GO nanosheets. (a) A schematic of the various functional groups present on the GO surface, (b) edge-group functionalization based on carboxyl and hydroxyl groups, and (c) basal-plane modification based on epoxide groups and the graphitic plane of GO.

poly(ethylene glycol) (PEG), polydiacetylenes (PDA), polyacrylamide (PAM), polyurethane (PU), and poly(methyl methacrylate) (PMMA).[46–48] Successful functionalization of the carboxylic acid groups on the GO nanosheets was confirmed *via* Fourier-transform infrared spectroscopy (FT-IR) and X-ray photoelectron spectroscopy (XPS) measurements. In the FT-IR spectra, the peak intensity of the carboxyl groups was considerably decreased after the coupling reaction with amines, whereby the peak at around 1640 cm^{-1} signified the formation of amide bonds. In addition, XPS measurements confirmed that distinct peaks of heteroatoms such as N and S appeared after functionalization, indicating the presence of the desired molecules covalently incorporated on the GO nanosheets.

Besides esterification or amide formation of carboxylic acid groups, the hydroxyl groups can be functionalized using coupling chemistry.[49] For example, Zhang group demonstrated that the hydroxyl group of GO could serve as the nucleophile and condense with the carboxylic acid using coupling chemistry. At first, hydroxyl groups can be capped with *S*-1-dodecyl-*S*′-(α,α′-dimethyl-α″-acetic acid)trithiocarbonate (DDAT) molecules through DCC coupling. After that, poly(*N*-vinylcarbazole) was grafted onto the DDAT-functionalized GO. Furthermore, the hydroxyl groups can react with trialkoxysilanes or alkyltrichlorosilanes to afford siloxy linkage.[50–52] It is also worth noting that Swager group reported the covalent functionalization of hydroxyl groups through a Claisen rearrangement (Fig. 2b).[53] Allylic alcohol groups are converted into vinyl allyl ethers by using *N*,*N*-dimethylamide groups that are then transformed into the corresponding carboxylate. As a result, these functionalized GO derivatives have dramatically increased solubility in aqueous media.

2.2 Basal plane modification

Another route for modifying GO is derivatization of the basal plane of GO nanosheets through ring-opening reactions involving epoxy functional groups with strong nucleophiles in polar solvents.[39] For example, Swager group demonstrated that malononitrile carbanions can form C–C bonds with the epoxy groups of GO (Fig. 2c).[54] Successful modification was confirmed *via* XPS analysis, which showed that N was incorporated at around 3.4% during the addition of malononitrile to GO and indicates that the alkyl nitrile groups were bound to the surfaces of the GO nanosheets. Similarly, ethylene glycol (EG) can be functionalized through the nucleophilic reaction between epoxy and hydroxyl groups under strongly basic conditions.[39] The functionalized GO derivatives exhibited two additional peaks at 2966 and 2865 cm^{-1} in FT-IR spectra, indicating asymmetric and symmetric stretching modes of C–H bonds from the ethylene spacer group in EG, respectively. In addition, atomic force microscopy (AFM) images demonstrate that the thickness of GO nanosheet after chemical modification was similar to that of pristine GO, reflecting the mild nature of this synthetic protocol.

Furthermore, highly reactive intermediates such as aryl diazonium salts, carbenes, and nitrenes can be directly functionalized on the aromatic basal plane of GO.[55] Especially, diazonium chemistry has been widely employed to functionalize the surface of graphene with aryl diazonium salts. Under acidic conditions, the diazonium salt forms an aryl cation by releasing N_2 gas, while the graphene lattice provides an electron for the aryl diazonium ion that is readily incorporated to the sp^2-carbon network.[56] Through this reaction, the sp^2 hybridization of basal plane could be changed to sp^3 upon functionalization. Tour group was the first to demonstrate that various aromatic moieties can be introduced on chemically reduced GO (rGO) nanosheets.[57] Since diazonium salts can react with the graphitic lattice on the basal plane of GO, pristine GO is reduced with hydrazine to recover the sp^2-hybridized graphitic lattice followed by chemical functionalization.[58] Functional groups of GO improved dispersion stability dramatically in DMF, NMP, and *N*,*N*′-dimethylacetamide (DMAC) even under centrifugation forces.[39]

Click chemistry has been successfully applied in material modification due to its advantages such as excellent functional group tolerance and high selectivity, quantitative yield, and high fidelity under mild experimental conditions with a wide range of chemical species.[59,60] In 2010, Wu group introduced the click chemistry to functionalize graphene.[61] First, azido-terminated polystyrene (PS) was prepared, and GO nanosheets were then functionalized by using propargyl alcohol through acylation. Then, the click reaction was proceeded between alkyne-functionalized GO and azido-terminated PS with copper bromide as the catalyst, which afforded PS-grafted GO nanosheets. After this early investigation, various molecules and polymers have since been anchored to the graphene nanosheets by exploiting click chemistry.[62–65]

As we have described in this section, a variety of organic transformations can be readily applied to realize the covalent functionalization of GO nanosheets *via* the introduction of various molecules.

3. Dispersibility

The dispersibility of GO in various aqueous and organic solvents is critical for expanding its potential for use in a wide variety of applications.[66] Although the rich oxygen functionality of GO enables its innate dispersion stability in aqueous media, it limits its dispersity in most non-polar organic solvents. To address this challenge, the covalent modification of the surface of GO nanosheets can offer stable GO dispersion in various solvents. The interactions between the solvents and the functional groups introduced reduces the intersheet hydrogen bonding and van der Waals forces between GO nanosheets, thereby increasing the colloidal stability in solvents. For example, sulfanilic acid group was chemically incorporated into GO nanosheets, which resulted in a superior dispersibility in water due to ionic repulsion. On the other hand, polar and non-polar groups introduced into GO nanosheets can induce dipole–dipole and van der Waals interaction with polar and non-polar solvents, respectively. The primary purpose of this section is to present the dispersion behavior of GO in various solvents in the context of

covalent functionalization. Specifically, the dispersion stability of GO in lubricating oils is also described, which is relevant to tribological applications of GO nanosheets, by exploiting the weak van der Waals interactions between adjacent graphene lamellae.

3.1 Aqueous suspension

GO prepared by using oxidizing graphite flakes with strong acid offers a layered morphology with various oxygen functionalities on the periphery of the graphitic planes that disrupt the stacking of multilayered GO nanosheets. Dispersions of the resulting highly functionalized GO are stable in aqueous solvents. However, when the oxygen functionalities are removed in the preparation of rGO, the graphene nanosheets lose their water solubility and eventually undergo irreversible aggregation. Therefore, additional processing steps are often required to produce aqueous dispersion with isolated graphene nanosheets.

Samulski and coworkers first reported chemical pathways toward producing isolated and sulfonated graphene that is soluble in aqueous media by reducing GO in two stages.[67] The pre-reduction of GO was carried out with sodium borohydride at 80 °C for 1 h to remove most of the oxygen-related functionality. After that, sulfonation of GO was then performed in an ice bath with an aryl diazonium salt of sulfanilic acid for 2 h, followed by post-reduction with hydrazine at 100 °C for 24 h to remove any remaining oxygen functionality. The highly negative charge of the sulfonate group was easily generated due to the very low pK_a (−6.62) of the sulfonic acid group inducing significant repulsion between the graphene nanosheets, thus preventing the graphene nanosheets from aggregating in aqueous media and improving aqueous dispersity.

Due to GO's good biocompatibility, excellent mechanical strength, and high electric conductivity, GO can be applied to biomedicine and clinical diagnostics such as biosensor[68–70] and bioenzyme electrodes.[71] Furthermore, GO can be applied to water splitting application due to its superior electron mobility. Therefore, in order to extend the application range of GO in biological and photocatalytic applications, it is important to modify the surface of GO to further increase solubility in water.

3.2 Non-aqueous suspension

The dispersibility of exfoliated GO was initially investigated to understand the interactive forces in different solvents.[66] GO can be dispersed in only a few solvents such as water and NMP, and is slightly soluble in DMF, and EG. The poor solubility of GO in organic solvents is due to the combination of highly polar surface functional groups and lamellar morphology that gradually leads to aggregation and precipitation. To mitigate this, the covalent functionalization of GO nanosheets with model compounds that resemble the chemical nature of the desired solvent is generally performed to improve the dispersion of GO. As a representative example, GO nanosheets can be chemically functionalized with ethanolamine (EA), ethylene glycol (EG), and sulfanilic acid (SA) to bestow excellent dispersion stability in the respective organic solvent, especially EG as a model coolant (Fig. 3a).[39] Specifically, carboxylic acids groups on the GO nanosheets react with amine groups in EA through

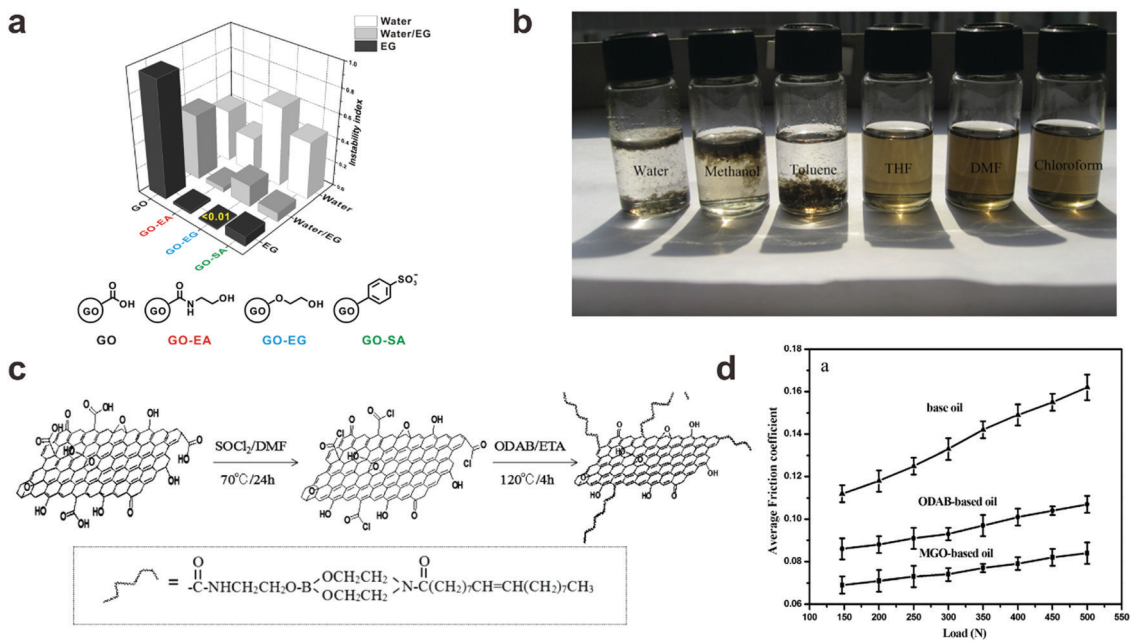

Fig. 3 (a) Schematic illustration and the instability index of covalently functionalized GO derivatives in water, a water/ethylene glycol (EG) mixture, and EG (reprinted with permission from ref. 39. Copyright 2016 American Chemical Society). (b) Dispersions of GO/PS in various organic solvents (reprinted with permission from ref. 73. Copyright 2011 Elsevier). (c) Schematic representation of the fabrication of oleic diethanolamide borate (ODAB)-grafted GO nanosheets (MGO) and (d) the average friction coefficient values of the base oil, ODAB-based oil, and MGO-based oil under different loads (reprinted with permission from ref. 90. Copyright 2017 American Chemical Society).

EDC-mediated surface modification. In parallel, GO functionalized with EG (GO-EG) can be synthesized by ring-opening of the epoxy groups with hydroxy groups under basic conditions. Sulfonated GO (GO-SA) was separately prepared by applying diazonium chemistry through directly anchoring sulfonic acid containing aryl radicals on the surface of the graphitic layer. The functionalized GO derivatives were successfully dispersed in EG at a concentration of 9.0 mg mL^{-1} (0.50 vol%). Especially, GO-EG and GO-EA showed enhanced dispersibility approximately 96 and 48 times higher than unreacted GO nanosheets, respectively, in EG.

Alkyl and aryl isocyanate modification of GO can induce stable dispersion in polar aprotic solvents by making the hydroxyl and carboxyl groups on the GO nanosheets into carbamate and amide groups, respectively.[72] In contrast to the parent GO, the isocyanate-treated GO is not dispersed in water at all. However, after a short ultrasonic treatment, stable colloidal dispersions can be readily formed in polar aprotic solvents such as DMF, NMP, dimethyl sulfoxide (DMSO), and hexamethylphosphoramide (HMPA). The phenyl isocyanate-treated GO in DMF forms the dark brown dispersion, which is stable for weeks without forming any visible precipitate.

Yang *et al.* modified graphite oxide with alkyne-terminated PS *via* click chemistry.[73] Azido-modified GO was synthesized *via* esterification and substitution of the hydroxyl groups on the surface of GO nanosheets. The PS-grafted graphene is obtained by grafting alkyne-functionalized PS onto the surface of the GO. The functionalized GO displayed excellent solubility in polar solvents such as THF, DMF, and chloroform (Fig. 3b). Besides these methods, the preparation paths for the target hydroxy-related functionalization of GO have been extended to enhance the dispersibility of GO in a variety of organic solvents.

As demonstrated by these examples, significant efforts have been directed toward the covalent functionalization of GO to afford the necessary solubility in organic solvents. These methods will open up further opportunities for a wide range of potential applications of GO nanosheets, such as organo-catalysts,[74,75] polymer composites,[76] and lubricant additives.[77,78] The dispersion stability coupled with the high surface area of the GO nanosheets presents the high catalytic efficiency of organic compounds.[79] Furthermore, the homogenous dispersion of functionalized GO in solvents and matrix polymers allows the incorporation of GO nanosheets as a conducting filler into polymer composites, resulting in excellent composites possessing high mechanical strength, electrical conductivity, and flexibility.[80] In addition, the dispersibility of alkylated GO in hydrocarbon solvents is observed to induce long-term dispersion stability in lubricating oil.[81] The weak van der Waals interactions between the atomic-thick lamellar structures of GO sheets reduce shear resistance and lower friction.[82] The examples of the application of GO as the lubricant additives are described more in the following section.

3.3 Tribological properties

Liquid lubricants are placed to sliding interfaces through oil delivery mechanisms, whereas solid lubricants are applied as thin films by using physical and/or chemical vapor deposition methods.[83] The solid lubricant films eventually wear out and lose lubricating effectiveness due to their finite thickness. In addition, they are more sensitive to oxygen, and humidity in the surrounding air, whereas the liquid lubricants are environmentally less sensitive and highly durable, making them more desirable as robust lubricants. Graphene can be potentially used as a lubricant due to its high surface area, superior mechanical strength, and excellent thermal conductivity. In particular, the weak van der Waals interactions between the lamellar structures of graphene play an important role when graphene is used as an additive to lower shear resistance and reduce friction.[84–86] However, the poor long-term dispersion stability of graphene in lubricating oils has created a major challenge for its use in the lubricant industry. This is because graphene tends to become agglomerated in most lubricants due to highly cohesive interactions and its poor dispersibility. As an alternative, chemically reactive GO can be applied as an additive *via* chemical functionalization to improve its dispersion stability in lubricating oils. For example, the grafting of long alkyl chains onto GO increases the dispersibility of the resulting modified GO in mineral and synthetic lubricating oils. The compatibility of GO in lubricants is primarily driven by the weak van der Waals force between the long alkyl chains grafted on GO and the hydrocarbon moiety of the lubricating base oil.[87]

The carboxyl groups in GO bestow tremendous potential for covalent functionalization with various oil-compatible organic moieties. Specifically, thionyl chloride used as a coupling agent with carboxylic groups can be selectively targeted for alkylamine grafting *via* amide linkage. The long alkyl chains of octadecylamine (ODA) modified GO (GO-ODA) provide sufficient cohesive interaction with hexadecane, leading to the uniform dispersion of GO-ODA in lubricating oil that, at a concentration of 0.06 mg mL^{-1}, decreased the coefficient of friction and wear scar diameter of hexadecane by 26% and 9%, respectively.[88] The enhanced tribological performance of GO-ODA was attributed to its uninterrupted presence between the steel ball and friction surface.

Khatri and coworkers also prepared GO-ODA that was well dispersible in lubricating oil.[89] Simultaneous reduction of the oxygen functional groups in GO restores the graphitic structure, and the resulting GO-ODA nanosheets at the contact interfaces not only protect the surface against tribo-damage from undesirable wear but also significantly reduce friction. In another approach, oleic diethanolamide borate (ODAB) has been selectively functionalized on GO through amide linkage (Fig. 3c).[90] The resultant GO-ODAB showed excellent dispersibility in the base oil, and using 0.02 wt% GO-ODAB between the steel ball and friction surface reduced the coefficient of friction and wear scar diameter by 38.4% and 42%, respectively (Fig. 3d).

Dodecyl chains were grafted on the surface of GO *via* click chemistry. Alkyne-functionalized GO is prepared *via* amide linkage with carboxylic acid groups of GO, followed by the click coupling between alkyne grafted GO and azidodecane. The resulting decane-functionalized GO as an additive for petroleum

lube oil enhanced the tribological properties by reducing the friction and wear by 16% and 30%, respectively.[91] Therefore, solid lubricant additives are very important for low friction and protection of contact surfaces, which can be achieved by dispersion of graphene nanosheets in the applicable lubrication oil.

Over the last decade, considerable efforts have been made for covalent functionalization of GO to achieve stable dispersion in lubrication oils, and the poor solubility of GO in lubricants has primarily been overcome by introducing hydrophobic chains like alkyl groups on the surface of the GO nanosheet. Thus, covalent chemical functionalization of GO can afford novel additives that are stably dispersible in lubricating oils.

4. Conductivity

Chemically oxidized GO nanosheets produced by oxidation and exfoliation has been difficult to apply in the field of electronic devices since GO itself exhibits low electrical properties due to the presence of various defect sites in the GO nanosheets.[48,92] As the oxygen content of GO increases, the sp^2 structure of GO is damaged, resulting in a decrease in electrical conductivity, particularly when the oxygen content exceeds 25 wt%.[21] To improve the electrical properties of GO by restoring the sp^2 network, many approaches have been reported to thermally or chemically reduce GO toward energy applications.

Meanwhile, the hydrophilic functional groups on the surface and edges of GO together with its large specific surface area improve the ionic conductivity.[93] By functionalization of GO, more interconnected ion transport channels can be provided,[94,95] and the ion transport pathway can be shortened by reducing interlayer interaction to further improve ionic conductivity.[96] In this section, we describe the examples of improving the electrical and/or ionic conductivity of GO through covalent functionalization toward its use in various applications such as supercapacitors, sensors, batteries, and flexible devices.[97]

4.1 Electrical conductivity

Kong and coworkers reported the covalent functionalization of reduced GO aerogel (RGOA) through diazotization and amidation to graft a conducting polymer, polyaniline (PANI) for capacitive material onto the surface of RGOA (Fig. 4a).[98] Covalent linkage between the RGOA and PANI enables not only to enhance electrical conductivity, but also to prevent the agglomeration of graphene nanosheets while increasing the surface area of the RGOA. As a result, the PANI-grafted RGOA exhibited higher capacitive performance (396 F g^{-1} at 10 A g^{-1}) than that of RGOA (183 F g^{-1} at 10 A g^{-1}). The PANI-grafted RGOA also

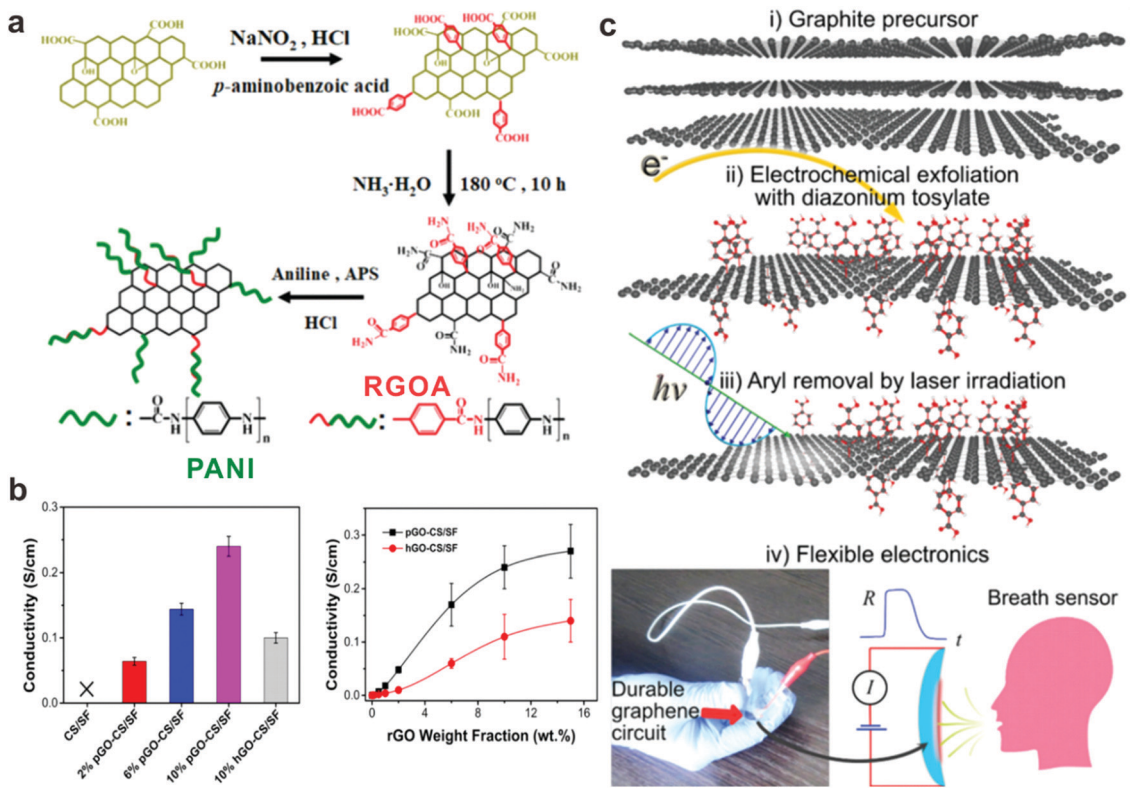

Fig. 4 (a) Preparation route of covalent functionalization of rGO aerogel (RGOA) with polyaniline (PANI) (reprinted with permission from ref. 98. Copyright 2019 Royal Society of Chemistry). (b) (left) Conductivity of scaffolds with various amounts of polydopamine-reduced GO (pGO) and hydrazine-reduced GO (hGO). (right) Electrical conductivity of scaffolds with varying pGO or hGO content (reprinted with permission from ref. 99. Copyright 2019 American Chemical Society). (c) Schematics of single-layer diazonium-functionalized graphene through laser processing (reprinted with permission from ref. 100. Copyright 2020 Royal Society of Chemistry).

demonstrated a high cycling stability of 56% capacitance retention after 4000 charge/discharge cycles at 10 A g^{-1}. These features showed that PANI-grafted RGOA is suitable for high-performance supercapacitor electrodes.

In another approach, Lu and coworkers fabricated polydopamine-reduced GO (pGO)-incorporated into a chitosan (CS) and silk fibroin (SF) scaffold (pGO-CS/SF) to develop an electroactive wound dressing that can respond to physiological electrical signals (Fig. 4b).[99] In this strategy, functionalized GO with the catechol moiety was reduced to pGO upon self-polymerization of dopamine, resulting in restoring the high conductivity of pGO. Inherently, CS/SF is non-conductive, but along with an increase in pGO content, the electrical conductivity of the CS/SF scaffold was increased significantly. Also, it is worth to note that pGO demonstrated higher conductivity than the control group using hydrazine-reduced GO (hGO), which only had the conductivity of 0.1 S cm^{-1}. Since pGO was well distributed in the scaffold along with the formation of electronic pathway, it resulted in improved electrical conductivity. The maximum conductivity of pGO-CS/SF reached 0.26 S cm^{-1}, which enables the transmittance of electric signals to regulate cellular activities.

Sheremet and co-workers produced single-layer diazonium-functionalized graphene through a strategy to improve electrical conductivity by cleaving *C*–aryl group bonds through laser irradiation (LMod-G) (Fig. 4c).[100] The strategy is unusual in that it differs from the conventional case of functionalized GO that becomes conductive owing to the removal of oxygen-containing groups and reduction. The cleavage of *C*–aryl group bonds *via* laser irradiation affected the transformation of sp^3-hybridized carbon structures to sp^2-hybridized network with the restoration of the conjugated carbon structure. As a result, diazonium-functionalized graphene with a low sp^3-carbon content was formed, and the electrons can flow freely through the LMod-G film, resulting in excellent electrical conductivity. The conductance of LMod-G with 2.7 mm thickness was 275.8 × 10^{-9} S. Due to this improved electrical conductivity, LMod-G showed significantly improved sensitivity of up to 15-fold than that of GO to breath (water vapor and CO_2) and the detection of ethanol, thereby demonstrating its applicability as a breath sensor.

4.2 Ionic conductivity

Kim *et al.* has produced ionic-liquid modified reduced GO (rGO-IL) nanosheets anchoring manganese oxide (Mn_3O_4) (Fig. 5a).[101]

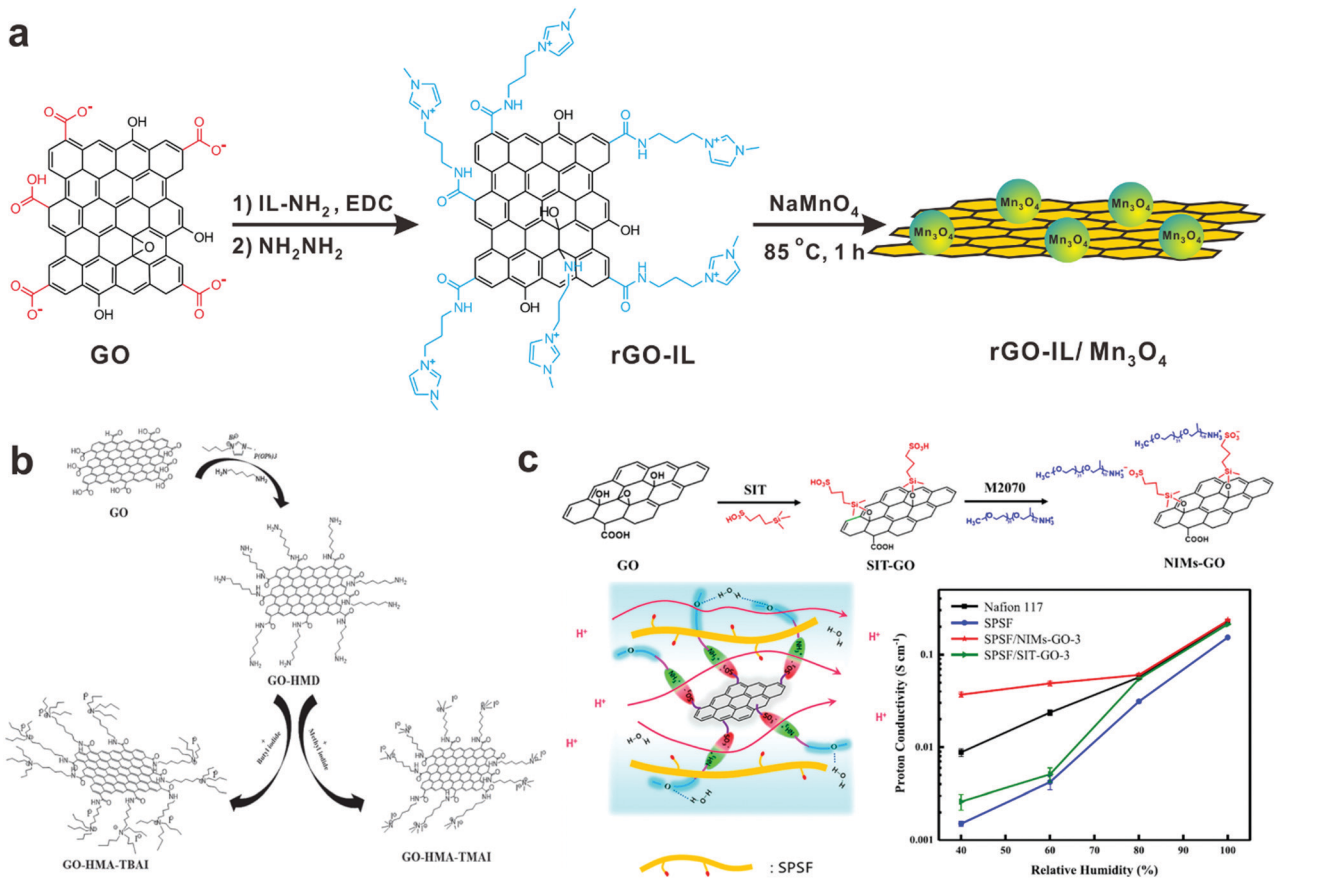

Fig. 5 (a) Schematic representation of the ionic-liquid modification of the surface of GO and the subsequent formation of manganese oxide nanoparticles (reprinted with permission from ref. 101. Copyright 2011 Royal Society of Chemistry). (b) Schematic illustrations of the formation of ionic-liquid-modified GO (GO-IL) and its derivatives (reprinted with permission from ref. 102. Copyright 2017 Elsevier). (c) Synthetic process of GO-based nanoscale ionic materials (NIM-GO) for application in proton exchange membranes with corresponding proton conductivity changes with respect to relative humidity (reprinted with permission from ref. 103. Copyright 2019 American Chemical Society).

The introduction of the ionic-liquid moiety increased the solubility of GO in a wide range of solvents, which can facilitate the separation of ionic groups. Hence, the ionic conductivity of GO was enhanced and Mn_3O_4 nanoparticles could easily grow onto the rGO-IL nanosheets *via* electrostatic interactions and hydrolysis. Especially, rGO-IL/Mn_3O_4 (10 : 1) nanoparticles displayed a surface resistance of 61.1 ohm sq^{-1}, indicating higher conductivity than rGO-IL/Mn_3O_4 (2 : 1) with a higher Mn_3O_4 ratio (52.5%), in which the surface resistance was 120.3 ohm sq^{-1}. Furthermore, rGO-IL/Mn_3O_4 (10 : 1) had a maximum peak power density of 120 mW cm^{-2}, showing the possibility of its application as a cathode material in Zn–air batteries.

Kowsari and Chirani prepared covalent ionic-liquid-functionalized GO (GO-IL) and its derivatives as a highly effective electrolyte additive for dye-sensitized solar cells (Fig. 5b).[102] They demonstrated that GO-IL formed a molecular bridge for electron transfer in the IL-based electrolyte due to the presence of polar alkyl chains improving the movement of free ions in an arranged pathway. As a result, the ionic conductivity improved by approximately two-fold to 3.14×10^{-4} S cm^{-1} when the GO-IL additive was used in the standard electrolyte.

In another notable example, Jiang and coworkers reported that the ionic conductivity of GO was improved by sulfonation (Fig. 5c).[103] In this study, GO was sulfonated with 3-(trihydroxysilyl)-1-propanesulfonic acid and subsequently neutralized with an amino-terminated polyoxypropylene-*b*-polyoxyethylene block copolymer (NIMs-GO). The synthesized NIMS-GO formed a very efficient proton-hopping site and a wide range of hydrogen-bonding networks by the introduction of sulfonic acid/amine acid–base pairs. In addition, owing to the introduction of the polyoxyethylene group, its water uptake and retention ability was enhanced even under low humidity operating conditions, and proton transfer occurred smoothly. Consequently, the NIMs-GO membrane exhibited a 52% increase in proton conductivity compared to a pristine sulfonated polysulfone membrane at 75 °C under 100% relative humidity, suggesting its high potential in the proton exchange membrane of fuel cells.

5. Catalytic activity

5.1 Carbocatalysts

In general, most previous studies have reported using GO as a platform to provide an anchoring site for active materials and to enhance catalytic activity. In this context, covalent functionalization can be used to introduce active ligands that can bind to metals and metal ions to improve catalytic performance. For example, our group reported GO functionalized with the mussel-inspired chemical moiety, dopamine (GO-Dopa).[104] The catechol groups of dopamine offer electrons for reducing Ag ions to form Ag nanoparticles on the surface of GO-Dopa. The resulting hybrid Ag/GO-Dopa was utilized as an organocatalyst that exhibited excellent catalytic activity in the reduction of nitroarenes.

Alternatively, GO and its derivatives are attracting considerable attention as promising metal-free heterogeneous catalysts owing to their high surface area, easy recyclability, and the variety of functional groups. In the case of pristine GO, its acidic and oxidative nature allows it to serve as a heterogeneous acid or oxidant.[105] In a pioneering study, Bielawski group showed that GO could serve as an efficient catalyst for the aerobic oxidation of benzylic hydrocarbons with high conversion (>98%) and selectivity (>95%) under mild conditions.[106] Moreover, the catalytic reactivity could be sustained for up to 10 cycles, albeit with a modest reduction after the first run.

Loh group further developed the application of GO in various organic reactions (Fig. 6a).[107] As a notable example,

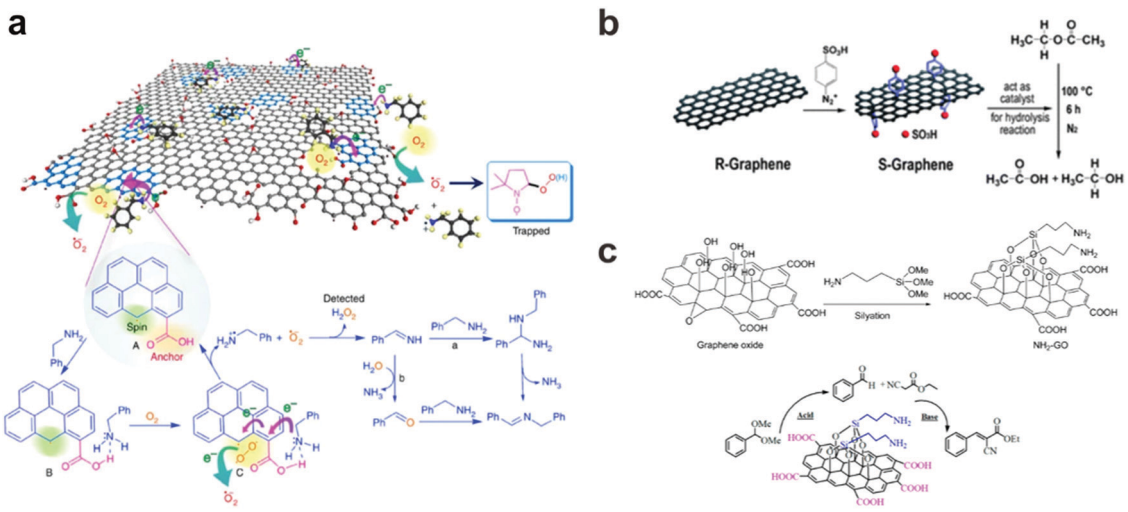

Fig. 6 Representative examples for GO-based carbocatalysts. (a) Base- and acid-treated GO (ba-GO) catalyzes the oxidative coupling of primary amines (reprinted with permission from ref. 107. Copyright 2012 Springer Nature). (b) Sulfonated GO as a solid catalyst for the hydrolysis of ethyl acetate (reprinted with permission from ref. 58. Copyright 2010 Royal Society of Chemistry). (c) Amine-functionalized GO for hydrolysis and Knoevenagel condensation (reprinted with permission from ref. 108. Copyright 2014 American Chemical Society).

they synthesized base- and acid-treated GO that displayed high catalytic activity for the aerobic oxidation of primary amines to their corresponding imines. Furthermore, the results from a mechanistic investigation performed on a model system suggest that carboxylic acid groups play a vital role in the catalytic reactions. These oxidation reactions with GO open the possibility of using it as the carbocatalyst for other aerobic oxidation reactions.

GO derivatives as heterogeneous catalysts can be engineered by covalent functionalization to anchor active sites (Table 1). Sulfonated GO (S-GO), which is functionalized with phenylsulfonic acid groups by diazonium chemistry, is a representative example of a heterogeneous acid catalyst due to its low pK_a value of −6.62 (Fig. 2).[39] It has been found that S-GO demonstrated high activity for the hydrolysis of ethyl acetate and could be recycled several times without chemical degradation (Fig. 6b).[58]

Li group first reported a GO-based acid–base bifunctional catalyst by using the intrinsic carboxylic acids on the edges and the amine groups post-grafted onto the GO basal surface (Fig. 6c).[108] Amine groups incorporated *via* silylation showed good catalytic activity in one-pot deacetalization-Knoevenagel cascade reactions. Since GO-based catalysts create isolated regions of acid–base functionality, they reacted independently with different reactants, resulting in high selectivity and yields. Further studies and the detailed utilization of GO derivatives as carbocatalysts are summarized in Table 1.

More recently, several groups have developed GO-based carbocatalysts for the multi-step conversion of biomass chemicals to value-added products.[109,110] Biomass feedstocks such as cellulose and biomass-derived substrates hold significant potential for future industrial applications. The application of efficient heterogeneous catalysts to transform biomass into valuable products is one of the main current challenges in green chemistry. In this context, reduced sulfonated GO obtained from the reaction of rGO using a sulfanilic acid diazonium salt intermediate was employed as an acid catalyst to produce furfural from xylose solution.[111] In addition, a reusable reduced sulfonated GO catalyst for the catalytic dehydration of xylose produced a high yield of furfural (~66%). Similarly, it has been reported that sulfonated GO can serve as a solid catalyst for the conversion of 5-hydroxymethylfurfural into biofuels such as alkyl levulinate and 5-alkoxymethylfurfural.[112] Compared to commercial catalysts (Amberlyst-15), the sulfonated GO produced a high yield with the necessary stability over consecutive catalytic runs.

As covered in this section, GO-based heterogeneous catalysts possess extraordinary advantages in terms of sustainability and tunability when designing the active catalytic centers to promote the desired catalytic reaction.

5.2 Photocatalysts

Efficient photocatalysts can be designed by combining photoresponsive materials with GO to accelerate photoreactions with electron–hole pair generation. Since the carrier mobility and high specific area of GO enables the efficient charge transfer in the hybrid material, GO has been applied for donor–acceptor hybrid materials with photoactive moieties. Thus, the notable electron mobility of GO can enhance the photocatalytic activity of conventional materials that suffer from rapid recombination of electron–hole pairs. In this section, we describe the photoresponsive properties of GO derivatives and their applications in photocatalysis and photovoltaics.

Ru complexes have been widely used as a photosensitizer due to their excellent photostability, light-harvesting capability, and efficient charge transport behavior. As a representative example, Jain group synthesized a heterogeneous photocatalyst comprising a GO-based Ru composite for the photocatalytic

Table 1 Catalytic reactions using GO and its derivatives as carbocatalysts

Catalyst	Reaction	Conditions	Yield (%)	Ref.
GO	Aerobic oxidation of alcohol	Catalysts 5–200 wt%, under air, 25–150 °C, 3–144 h	98	Dreyer *et al.*[106]
GO	Aza-Michael addition of amines	Catalyst 0.025 mg, amine 1 mmol, unsaturated compounds 1.2 mmol, room temperature, 30 min	97	Vermar *et al.*[113]
GO	Friedel–Crafts reactions	Catalyst 3 wt%, room temperature, styrene oxide 1.0 mmol, indole 1.2 mmol, 96 h	80	Acocella *et al.*[114]
Base- and acid-treated GO	Oxidative coupling of amines	Catalyst 5 wt%, amine 1 g, under air, 90 °C, 12 h.	98	Su *et al.*[107]
Sulfonated GO	Ring-opening of epoxides	Catalyst 5 mg, substrate 1 mL, methanol 10 mL, room temperature, 1–24 h	99	Dhakshinamoorthy *et al.*[115]
Sulfonated GO	Dehydration of xylose	Catalyst 2 wt%, under air, 200 °C, 35 min	62	Lam *et al.*[111]
Sulfonated GO	Hydrolysis of ethyl acetate	Catalyst 20 mg, ethyl acetate 0.375 mL, under air, 70 °C, 6 h	64	Ji *et al.*[58]
Sulfonated GO	Transesterification	Catalyst 5 wt%, under air, 150 °C, 2–4 h	93	Wang *et al.*[116]
Sulfonated GO	Conversion of 5-hydroxy methylfurfural.	Catalyst 10 wt%, 0.33 M HMF, under air, 110–140 °C	94	Antunes *et al.*[112]
Sulfonated GO	Conversion of glucose to 5-hydroxy methylfurfural	Catalyst 60 mg, glucose 10 wt%, under air, 170 °C, 2 h	19.5	Li *et al.*[117]
Amine-functionalized GO	Acetal hydrolysis and condensation	Catalyst 0.080 mmol, benzaldehyde dimethyl acetal 0.5 mmol, ethyl cyanoacetate 0.60 mmol, toluene 5.0 mL, 80 °C, 3 h	95	Dhakshinamoorthy *et al.*[118]
Amine and sulfonic acid-functionalized GO	Deacetalization-nitroaldol reaction	Catalyst 40 mg, benzaldehyde dimethyl acetal 2 mmol, nitromethane 10 mL, 90 °C, under N_2, 4 h	95	Li *et al.*[119]

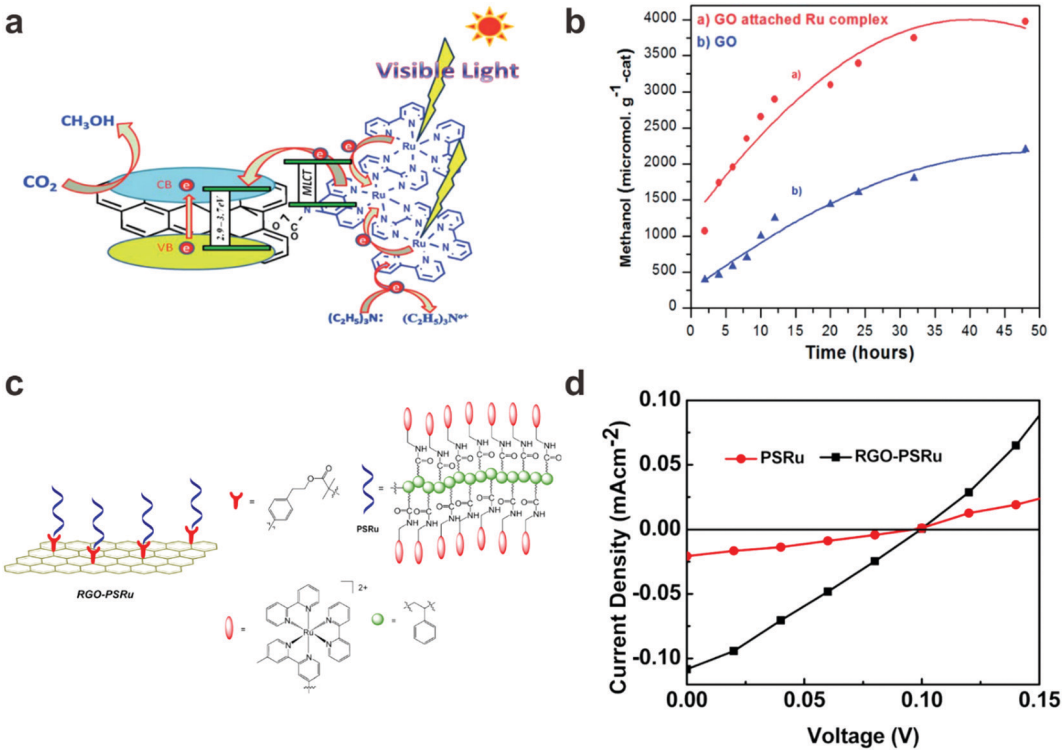

Fig. 7 (a) Possible mechanisms of the photocatalytic reduction by GO with an Ru-based photocatalyst (reprinted with permission from ref. 120. Copyright 2014 Royal Society of Chemistry). (b) Conversion of CO_2 to methanol using a GO-based Ru complex (reprinted with permission from ref. 120. Copyright 2014 Royal Society of Chemistry). (c) Schematic representation of a reduced GO-PS based Ru composite (RGO-PSRu) (reprinted with permission from ref. 122. Copyright 2013 American Chemical Society). (d) Current density–voltage curves of RGO-PSRu/$PC_{60}BM$/Al (reprinted with permission from ref. 122. Copyright 2013 American Chemical Society).

CO_2 reduction to methanol under visible light irradiation (Fig. 7a).[120] Specifically, the trinuclear Ru complex based on phenanthroline ligands was grafted onto the carboxylic acid group on the GO surface. The Ru complex facilitates the transportation of photoinduced electrons from it to the conduction band of GO. As a result, the GO–Ru complex displayed a reduction in the CO_2 to methanol yield of 3977.57 ± 5.60 μmol g_{cat}^{-1} under a 20 W white cold LED, which is a higher photocatalytic performance than GO without the Ru complex (Fig. 7b). In addition, these catalysts could be easily recovered and reused for 4 subsequent runs without a significant loss of catalytic activity.

In another approach, Yao *et al.* synthesized a photocatalyst consisting of rGO nanosheets as an electron acceptor and covalent organic frameworks (COFs) as a photoactive material (rGO-COF) *via* the facile grafting of phenylenediamine to rGO, which was then incorporated into the synthetic process for the COFs.[121] The resulting rGO-COF showed an enhanced H_2 evolution rate of 11.98 mmol g^{-1} h under visible-light irradiation, which was 4.85 and 2.50 times higher than pure COF and GO/COF without any covalent coupling between the two components, respectively. The enhanced photocatalytic property was attributed to the covalently grafted rGO in the composite that not only promotes the separation of photogenerated charges as an electron acceptor but also serves as an active electron transporter. Furthermore, the uniform morphology of the evenly distributed COFs on the layered rGO nanosheets can facilitate the migration of photoexcited electrons.

Fang and coworkers reported that rGO nanosheets grafted with polypyridyl-Ru-derivatized polystyrene (PS-Ru) exhibited enhanced photocurrent and power conversion efficiency over five-fold higher than those of devices without rGO (Fig. 7c and d).[122] Ru(II) polypyridine derivatized polymer was formed from methyl bromoisobutyrate initiation units on the hydroxyl group of rGO by atom transfer radical polymerization. The graphene moiety in the hybrid material acted as an excellent supporting matrix for the photo-responsive Ru complexes as well as offering superior electron transfer to suppress the recombination of photoinduced charges.

Furthermore, Vinoth *et al.* synthesized a hybrid material consisting of rGO and Ru complex with polyaniline (PANI–Ru) that was grafted onto the hydroxyl groups of the rGO nanosheets *via* covalent functionalization to afford rGO/PANI–Ru.[123] The chemical connection between PANI–Ru and rGO facilitates the photogenerated electron transfer from the Ru complex to rGO through the backbone of the conjugated PANI polymer chains. Polymer solar cells fabricated with rGO/PANI–Ru attained an almost 6-fold and 2-fold improvement in open circuit potential (V_{oc}) and short circuit current density (J_{sc}) compared to the control device using PANI–Ru without rGO under the illumination of AM1.5G. The superior electron transfer and charge separation characteristics of rGO further

Table 2 Photocatalytic reactions of GO functionalized with photosensitive materials

Covalent functionalization	Application	Role of GO	Performance	Ref.
Co phthalocyanine	Photoreduction of CO_2 into methanol	Electron acceptor	Enhanced methanol conversion rate over pristine GO (3781.8881 μmol g^{-1})	Kumar *et al.*[124]
Ru trinuclear polyazine complex	Photoreduction of CO_2 into methanol	Electron acceptor	Enhanced methanol conversion rate over pristine GO (3977.57 ± 5.60 μmol g^{-1})	Kumar *et al.*[120]
Heteroleptic Ru complex	Photoreduction of CO_2 into methanol	Electron acceptor	Enhanced methanol conversion rate over pristine GO (2050 μmol g^{-1})	Kumar *et al.*[125]
Re-2,2′-bipyridine complex	Photoreduction of CO_2 into CO	Electron acceptor	Enhanced photocatalytic efficiency and photostability for the conversion of CO_2 into CO (total turnover number ≥ 580)	Tian *et al.*[126]
Covalent organic frameworks	H_2 evolution reaction	Electron acceptor	Enhanced H_2 evolution rate (11.98 mol g^{-1} h^{-1}); 4.85 and 2.50 times higher than pure COF and rGO/COF without covalent connection	Yao *et al.*[121]
Polypyridyl-Ru-derivatized polystyrene	Photovoltaic cell	Electron acceptor	Enhanced photocurrent relative to devices without rGO (0.11 mA cm^{-2})	Fang *et al.*[122]
Pyridyl benzimidazole-based Ru complex coated with polyaniline	Photovoltaic cell	Electron acceptor	Enhanced open circuit potential (0.19 V) and short circuit current density (0.03 mA cm^{-2}) over the standard device made without rGO	Vinoth *et al.*[123]

promoted the electron injection from PANI–Ru to phenyl-C_{61}-butyric acid methyl ester ($PC_{60}BM$) acting as an electron acceptor polymer that consequently improved the overall performance of the polymer solar cells.

These several outstanding examples demonstrate that covalent functionalization chemistry on the surface of GO can enhance photocatalytic activity by combining it with photoactive materials, resulting in the synergistic effect of functional moieties and an efficient charge transfer capacity. Combining various photo-responsive materials with GO will possibly expand GO's potential for use in a wider range of applications (Table 2).

5.3 Electrocatalysts

To overcome energy crises and environmental pollution, numerous efforts have been devoted to alternative and renewable energy that can be substituted for conventional fossil fuel-based energy system. One promising solution is the utilization of key electrochemical energy conversion reactions, including oxygen evolution reaction (OER), hydrogen evolution reaction (HER), oxygen reduction reaction (ORR), carbon dioxide reduction reaction (CO_2RR), and nitrogen reduction reaction (NRR).[127,128] Typically, electrocatalysts based on noble metals such as Pt, Ir, and Ru have been widely used for these electrochemical reactions. In particular, Pt/C catalyst is the most widely used commercially owing to its excellent adsorption and charge transfer.[129,130] However, there are still some challenges concerning the high cost, low selectivity, poor stability, and vulnerability to gas poisoning.[131,132] Therefore, significant research endeavor has been devoted to fabricating alternative electrocatalysts with high abundance, excellent efficiency, and good stability.

In this context, modified GO has stood as a new class of metal-free electrocatalyst. Various oxygen- and nitrogen-containing groups in GO can absorb the active reactant and transfer electrons at the electrode interface.[127,133] In this section, we will introduce examples of improving electrocatalytic performance by modification of GO. The quantitative comparison of catalyst performance through parameters such as overpotential, Tafel slope, and limiting current density with pristine GO or commercial Pt/C catalysts is also presented (Table 3).

5.3.1 Functionalized GO electrocatalysts. The chemical functionalization of GO can further improve its chemical, electrical, and physical properties without compromising the intrinsic properties of the graphene structure.[134] In addition, functionalization can open the band gap by controlling the conjugation length of the delocalized carbon lattice, thus improving the electronic properties and catalytic activity.[135,136] It is also possible to precisely control changes in the characteristics according to site-specific reactions and to introduce heterogeneous functional structures.[137]

In particular, many studies have reported improving the electrocatalytic activity of GO by covalent functionalization with N-containing functional groups such as amino acids and amines that are more nucleophilic than the oxygen atoms in GO. Hence, interfacial bonding between GO and the substance of interest increases after functionalization. Thus, the functionalization of GO increases the number of active sites and endows superb electrocatalytic performance.[138] As an example of introducing an amino acid, Sathe and coworkers used L-lysine-functionalized rGO (Ly-rGO) as a catalyst for OER.[139] The increased number of active sites in the Ly-rGO electrocatalyst effectively adsorbed OH^- species from water and removed electrons to form intermediates. As a result, Ly-rGO exhibited improved OER properties compared to GO. For example, the overpotential of 330 mV for Ly-rGO was lower than that for GO of 650 mV at a current density of 10 mA cm^{-2}. In addition, a lower Tafel slope of 80 mV dec^{-1} was observed in Ly-rGO compared to GO of 88 mV dec^{-1}.

As an example of introducing an amine, Kim and Ahmed prepared the porous rGO catalysts with different linkages to prepare rGO-sp^2-rGO and rGO-sp^3-rGO, through covalent amidation with sp^3-hybridized 1,4-diaminobutane and sp^2-hybridized 1,4-diaminobenzene, respectively (Fig. 8a).[140] Each type of linkage was used as a junction between the rGO layers to improve the electrocatalytic activity for ORR resulting from interlayer charge transfer. rGO-sp^3-rGO was more active than rGO-sp^2-rGO in terms of ORR performance due to improved

Table 3 Representative catalytic reactions of functionalized GO as electrocatalysts

Type	Component	Effect	Catalytic performance	Reaction	Ref.
Covalent functionalization	Lysine	Enhances the number of catalytic active sites *via* increasing N-containing groups	Overpotential: 330 mV at 10 mA cm^{-2} Tafel slope: 80 mV dec^{-1} Excellent current stability for 5000 s	OER[a]	Sapner *et al.*[139]
	Tyramine	Enhances the number of catalytic active sites where hydroxyl radicals can be adsorbed	Onset potential: ~1390 mV *vs.* RHE Overpotential: 176 mV at 2 mA cm^{-2} Tafel slope: 69 mV dec^{-1}	OER[a]	Sapner *et al.*[127]
	Metallophthalocyanine polymer	Provides an electron transport bridge and a large specific surface area	Overpotential: 210 mV at 1 mA cm^{-2} Tafel slope: 216 mV dec^{-1} Double-layer capacitance: 203 mF cm^{-2}	HER[b]	Wang *et al.*[152]
	Pyridine	Enhances the number of catalytic active sites *via* increasing N-containing groups	Peak potential: −280 mV Number of electrons: 3.74	ORR[c]	Ensafi *et al.*[153]
	Ammonia	Enhances the number of catalytic active sites *via* increasing amine groups	Onset potential: −70 mV Peak current density: 1.15 mA cm^{-2}	ORR[c]	Navaee and Salimi[138]
	1,4-Diaminobutane, 1,4-diaminobenzene	Enhances the number of catalytic active sites *via* increasing N-containing groups	Peak potential: −280 mV Peak current density: 0.71 mA cm^{-2} Onset potential: −100 mV Number of electrons: 3.95–3.98	ORR[c]	Ahmed and Kim[140]
	Monothiol	Enhances chemical and physical properties *via* the introduction of S	Onset potential: 45 mV	ORR[c]	Chua and Pumera[134]
	Terpyridine	Induces intermolecular charge transfer	Number of electrons: 3.63–3.92	ORR[c]	Song *et al.*[154]
	Pyridine	Induces paramagnetic centers *via* the formation of aryloxy radicals	Onset potential: −87 mV *vs.* SCE Current density: −4.5 mA cm^{-2} Number of electrons: ~4	ORR[c]	Jahan *et al.*[155]
	Pyridine derivative	Enhances the number of catalytic active sites *via* the introduction of pyridinic-N	Faradaic efficiency: 45.8%	CRR[d]	Yuan *et al.*[141]
	Polydopamine	Adds N and S during post-modification	Difference between OER and ORR metrics: 880 mV	OER,[a] ORR[c]	Qu *et al.*[156]
Doping	Pyridinic-N-doped	Enhances the number of catalytic active sites and the absorption of hydrogen	Tafel slope: 100.56 mV dec^{-1}	HER[b]	Zheng *et al.*[147]
	N and S co-doped	Provides a fast electron transfer path *via* co-doping with N and S	Operating potential: −560 mV Tafel slope: 105 mV dec^{-1}	HER[b]	Ito *et al.*[157]
	N-Doped	Introduces a metal@carbon core–shell structure	Onset potential: −14 mV Overpotential: 70 mV at −10 mA cm^{-2} Tafel slope: 64 mV dec^{-1}	HER[b]	Jiang *et al.*[158]
	N-Doped	Forms microporous holes that lead to edge defects	Onset potential: ~1100 mV Half-wave potential: 840 V *vs.* RHE	ORR[c]	Dumont *et al.*[159]
	B-Doped	Introduces electron-deficient B-doped sites for strong N_2 adsorption	NH_3 production rate: 9.8 μg $(h{\cdot}cm^2)^{-1}$ Faradic efficiency: 10.8%	NRR[e]	Yu *et al.*[150]
	Ni-N-Modified	Enhances the number of catalytic active sites *via* the introduction of N moieties	Faradaic efficiency: 90% Tafel slope: 126 mV dec^{-1}	CRR[d]	Su *et al.*[160]
	N and P dual-doped	Enhances charge delocalization and introduces a hierarchically porous structure	Difference between the OER and ORR potentials: 710 mV	OER,[a] ORR[c]	Li *et al.*[151]
	N-Doped	Facilitates the formation of graphitic N	Kinetic-limiting current: 9.0 mA cm^{-2} at −400 mV Number of electrons: 3.8	OER,[a] ORR[c]	Li *et al.*[161]

[a] OER: oxygen evolution reaction. [b] HER: hydrogen evolution reaction. [c] ORR: oxygen reduction reaction. [d] CO_2RR: CO_2 reduction reaction. [e] NRR: N_2 reduction reaction.

specific surface area, a hierarchical porous structure, and π-electron interaction-free interlayer charge transfer. rGO-sp^3-rGO attained an excellent current density of 0.71 mA cm^{-2} and an onset potential of −100 mV, with a 1.4-times higher limiting diffusion

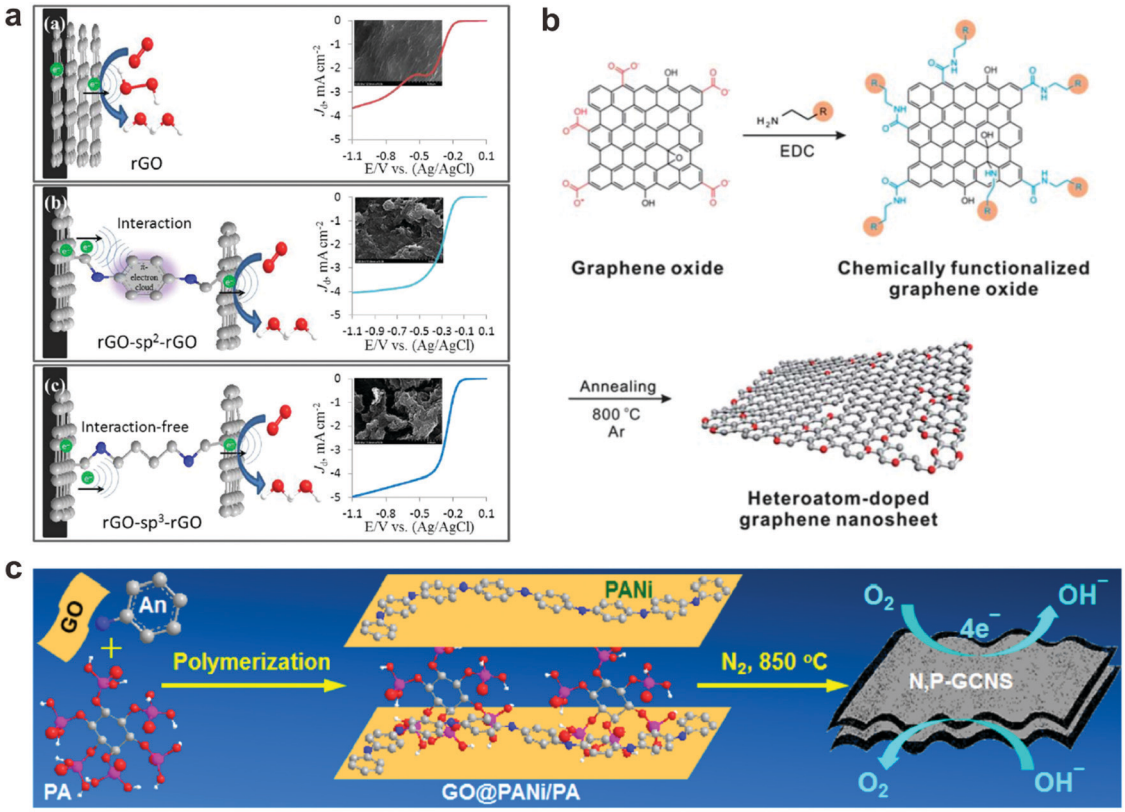

Fig. 8 (a) Proposed oxygen reduction reaction (ORR) mechanism on the surface of various rGO-based electrocatalysts (reprinted with permission from ref. 140. Copyright 2017 Springer Nature). (b) Schematic representation of covalent functionalization and subsequent thermal treatment of GO (reprinted with permission from ref. 41. Copyright 2013 Royal Society of Chemistry). (c) Schematic illustration of the bifunctional N and P dual-doped graphene/carbon nanosheets (N,P-GCNS) oxygen electrocatalyst (reprinted with permission from ref. 151. Copyright 2015 American Chemical Society).

current density than non-functionalized rGO. Furthermore, rGO-sp^3-rGO posed the potential to replace the commercial Pt/C catalyst with a Tafel slope of 61 mV dec^{-1}, similar to commercial Pt/C of 60 mV dec^{-1}. In terms of stability, the rGO-sp^3-rGO catalyst indicated a high relative current value of 88.5% even after 30 000 s, while the Pt/C catalyst showed a gradual decrease with a current loss of 57% under the identical period.

Lu and coworkers fabricated functionalized GO with five different pyridine derivatives: pyridoxine, 4-hydroxypyridine, 4-aminopyridine, 8-hydroxyquionline, and 5-amino-1,10-phenanthroline.[141] Pyridinic-N has a lone pair of electrons capable of binding with CO_2, and a high electron density that hinders the formation of CO, thereby reducing CO_2 to ethanol. Above all, since pyridoxine contains strong electron-donating groups such as –OH and –CH_3, functionalization with pyridoxine can increase the electronegativity of pyridinic-N. Remarkably, GO modified with pyridoxine demonstrated an optimal catalytic ability for the electrochemical reduction of CO_2 to ethanol with an overall faradaic efficiency that reached 45.8% unlike pristine GO with no catalytic activity.

Several researchers have also reported heteroatom-doped GO as efficient electrocatalysts synthesized through covalent functionalization using various small organic molecules and subsequent thermal treatment. For example, a series of N-doped rGO (NRGO) was synthesized to utilize as the electrocatalysts for ORR.[41] NRGOs were synthesized according to the following sequence (Fig. 8b). First, five sources of amine molecules (ethylene diamine, diethylene triamine, triethylene tetramine, tetraethylene pentamine, and pentaethylene hexamine) were introduced into GO based on the EDC-mediated reaction between the carboxylic acid groups of GO and the amine moiety in the small molecules. Subsequent thermal annealing treatment caused atomic rearrangement that led to the incorporation of N atoms from the functionalized amine groups into the graphene matrix. The prepared NRGOs exhibited excellent electrocatalytic activity through an efficient one-step, four-electron pathway as value as commercial Pt/C catalysts. This can be attributed to the charge polarization of the carbon network induced by the heteroatoms. In particular, NRGO synthesized using triethylenetetramine showed the most positive onset potential of −150 mV and the highest limiting current density of −4.55 mA cm^{-2}, along with the best ORR catalytic activity. This is because the corresponding NRGO has the most abundant pyridine-N functional groups, which are known to be active catalytic sites for ORR due to the delocalization of π-electrons. In addition, in an alkaline environment, NRGO showed a high current retention rate of 73% even after 10 000 s, showing a slower attenuation than Pt/C of 60%.

5.3.2 Doped-GO electrocatalysts. Like the aforementioned NRGO example, heteroatom-doped GO has been extensively

investigated in the field of electrocatalysis because the heteroatom doping of GO can modulate the charge distribution over the carbon network and improve the active sites on the GO surface *via* the charge polarization effect.[142,143] The chemical modification for electrocatalysis can be separated into chemical functionalization and doping, where the former involves the covalent attachment of functional groups and the latter involves the replacement of an element in the crystal lattice of the material.[134]

As a representative example of the N-doped GO as an electrocatalyst, Qiao and coworkers reported a metal-free electrocatalyst based on graphitic-carbon nitride and N-doped rGO.[144] The N-doping led to a sufficiently high positive charge density for the surrounding carbon atoms due to the large electronegativity difference between N (3.04) and C (2.55), resulting in polarization in the carbon network. The N-doped active sites in the carbon lattice promote the chemical adsorption of substances such as O_2 that enhances reactions such as ORR and HER.[145,146] Du and coworkers also reported N-doped GO electrocatalysts for HER formed with abundant pyridinic-N dopants by using laser irradiation.[147] The overpotential at the current density of 10 mA cm^{-2} was considerably reduced by over 400 mV in the N-doped GO compared with that of pristine GO. Furthermore, N-doped GO had a low Tafel slope of 100.56 mV dec^{-1}. This improved electrochemical HER performance resulted from the high pyridinic-N ratio, which increases the adsorption of H_2 and the number of potential active sites.

On the other hand, B-doping induces p-type conductivity in GO because B atoms are less electronegative than C atoms. Therefore, polarized B atoms act as adsorption sites for O_2 or N_2 molecules.[148,149] As a notable example, Yu *et al.* reported B-doped graphene fabricated by thermal annealing of GO and boric acid for NRR electrocatalysis.[150] Since N_2 is a weak Lewis base, it is ideal for creating Lewis acid catalytic sites with empty orbitals. They demonstrated that by introducing B as a dopant into the graphene structure, the local electron-deficient environment at the B-doped sites provides a strong binding site for Lewis bases, thereby greatly increasing N_2 adsorption. This B-doped graphene showed an excellent production rate of 9.8 μg h^{-1} cm^{-2} and high faradaic efficiency for NH_3 production of 10.8% at −500 mV *vs.* RHE, which was five to ten times higher than those of the undoped graphene.

Recent studies have also shown that binary or multiple-heteroatom-doped GO can provide a cost-effective strategy for producing multifunctional electrocatalysts. This is due to the synergistic effects arising from the electronic interactions among the different dopants.[142] For example, Gou and coworkers reported N and P dual-doped graphene/carbon nanosheets (N,P-GCNS) by direct pyrolysis of a polymer gel composed of GO, PANI, and phytic acid (PA) (Fig. 8c).[151] Dual-doping in N,P-GCNS enhanced the charge delocalization and asymmetric spin density of carbon atoms, resulting in the creation of more active sites. Moreover, it showed rapid kinetics for promoting O_2 and OH^- transportation owing to its hierarchically porous structure. As a result, as-prepared N,P-GCNS demonstrated superior bifunctional performance for ORR with an oxygen reduction current density of 2.24 mA cm^{-2}, an electron transfer number of 3.96, and a Tafel slope of 51 mV dec^{-1} as well as remarkable OER activity with an onset potential of −130 mV and OER current density of 70.75 mA cm^{-2}. N,P-GCNS showed better tolerance to methanol and CO and durability compared to Pt/C. Unlike Pt/C, the bifunctional catalyst showed little change in current density. Moreover, N,P-GCNS demonstrated a slight performance attenuation of 4.5%, whereas Pt/C showed a sharp current loss of 25.9%.

6. Summary and outlook

In this review, we presented controllable physicochemical characteristics of versatile GO scaffolds, such as dispersibility, mechanical strength, conductivity, and catalytic active sites, through covalent functionalization with various molecules and polymers *via* the oxygen-containing chemical functional groups on the edges and basal plane of GO. Without chemical functionalization and hybridization with other counterparts, the simple reduction of GO still poses limitations on acquiring the physical and chemical properties required for various practical applications. On the other hand, the introduction of covalently bonded chemical functionalities to GO can offer a convenient access to functionalized GO nanosheets by introducing desired molecules for target specific properties for various applications, which in turn, can result in high catalytic activity and the development of practical devices.

While there have been tremendous efforts and progress in the fundamental research and technological development of graphene-based materials in diverse fields, there are still some challenges to overcome in the field of functionalization of GO. For example, the preparation of homogeneous and highly reproducible GO samples and a method of accurately accessing the type and stoichiometry of surface functional groups as a single molecular entity remain considerable challenges. With the advances of the novel synthetic protocols and separation techniques such as a bottom-up approach[162] using radical addition reactions and more accurate separation techniques beyond current size filtration[163,164] and centrifugation method[165] to prepare GO nanosheets with defined structures and compositions, we envision there will be enormous opportunities remains to be explored in the future.

Author contributions

All authors contributed to the discussion of contents and the editing of the manuscript prior to submission. M. P., M. G., and B.-S. K. conceptualized the article. M. P. researched data related to covalent functionalization and carbocatalysts. N. K. researched data related to dispersibility, and photocatalysts. J. L. researched data related to conductivity and electrocatalysts.

Conflicts of interest

There are no conflicts to declare.

Acknowledgements

This work was supported by the National Research Foundation of Korea (NRF-2017M3A7B4052802 and NRF-2018R1A5A1025208).

References

1 M.-M. Titirici, R. J. White, N. Brun, V. L. Budarin, D. S. Su, F. del Monte, J. H. Clark and M. J. MacLachlan, Sustainable carbon materials, *Chem. Soc. Rev.*, 2015, **44**, 250–290.
2 A. H. Castro Neto, The carbon new age, *Mater. Today*, 2010, **13**, 12–17.
3 X. Duan, H. Sun and S. Wang, Metal-free carbocatalysis in advanced oxidation reactions, *Acc. Chem. Res.*, 2018, **51**, 678–687.
4 H. Wang, Y. Shao, S. Mei, Y. Lu, M. Zhang, J.-K. Sun, K. Matyjaszewski, M. Antonietti and J. Yuan, Polymer-derived heteroatom-doped porous carbon materials, *Chem. Rev.*, 2020, **120**, 9363–9419.
5 A. K. Geim, Graphene: Status and prospects, *Science*, 2009, **324**, 1530–1534.
6 K. S. Novoselov, V. I. Fal′ko, L. Colombo, P. R. Gellert, M. G. Schwab and K. Kim, A roadmap for graphene, *Nature*, 2012, **490**, 192–200.
7 A. K. Geim and K. S. Novoselov, The rise of graphene, *Nat. Mater.*, 2007, **6**, 183–191.
8 C. N. R. Rao, K. Biswas, K. S. Subrahmanyam and A. Govindaraj, Graphene, the new nanocarbon, *J. Mater. Chem.*, 2009, **19**, 2457–2469.
9 V. Georgakilas, J. N. Tiwari, K. C. Kemp, J. A. Perman, A. B. Bourlinos, K. S. Kim and R. Zboril, Noncovalent functionalization of graphene and graphene oxide for energy materials, biosensing, catalytic, and biomedical applications, *Chem. Rev.*, 2016, **116**, 5464–5519.
10 J. A. Mann, J. Rodríguez-López, H. D. Abruña and W. R. Dichtel, Multivalent binding motifs for the noncovalent functionalization of graphene, *J. Am. Chem. Soc.*, 2011, **133**, 17614–17617.
11 B. Long, M. Manning, M. Burke, B. N. Szafranek, G. Visimberga, D. Thompson, J. C. Greer, I. M. Povey, J. MacHale, G. Lejosne, D. Neumaier and A. J. Quinn, Non-covalent functionalization of graphene using self-assembly of alkane-amines, *Adv. Funct. Mater.*, 2012, **22**, 717–725.
12 J. A. Mann and W. R. Dichtel, Noncovalent functionalization of graphene by molecular and polymeric adsorbates, *J. Phys. Chem. Lett.*, 2013, **4**, 2649–2657.
13 Y. Xu, H. Bai, G. Lu, C. Li and G. Shi, Flexible graphene films via the filtration of water-soluble noncovalent functionalized graphene sheets, *J. Am. Chem. Soc.*, 2008, **130**, 5856–5857.
14 H. Zhou, A. Uysal, D. M. Anjos, Y. Cai, S. H. Overbury, M. Neurock, J. K. McDonough, Y. Gogotsi and P. Fenter, Understanding defect-stabilized noncovalent functionalization of graphene, *Adv. Mater. Interfaces*, 2015, **2**, 1500277.
15 A. Ghosh, K. V. Rao, S. J. George and C. N. R. Rao, Noncovalent functionalization, exfoliation, and solubilization of graphene in water by employing a fluorescent coronene carboxylate, *Chem. – Eur. J.*, 2010, **16**, 2700–2704.
16 S. Gilje, S. Han, M. Wang, K. L. Wang and R. B. Kaner, A chemical route to graphene for device applications, *Nano Lett.*, 2007, **7**, 3394–3398.
17 V. V. Neklyudov, N. R. Khafizov, I. A. Sedov and A. M. Dimiev, New insights into the solubility of graphene oxide in water and alcohols, *Phys. Chem. Chem. Phys.*, 2017, **19**, 17000–17008.
18 C. K. Chua and M. Pumera, Covalent chemistry on graphene, *Chem. Soc. Rev.*, 2013, **42**, 3222–3233.
19 S. Eigler and A. Hirsch, Chemistry with graphene and graphene oxide—challenges for synthetic chemists, *Angew. Chem., Int. Ed.*, 2014, **53**, 7720–7738.
20 W. S. Hummers and R. E. Offeman, Preparation of graphitic oxide, *J. Am. Chem. Soc.*, 1958, **80**, 1339.
21 D. C. Marcano, D. V. Kosynkin, J. M. Berlin, A. Sinitskii, Z. Sun, A. Slesarev, L. B. Alemany, W. Lu and J. M. Tour, Improved synthesis of graphene oxide, *ACS Nano*, 2010, **4**, 4806–4814.
22 D. R. Dreyer, S. Park, C. W. Bielawski and R. S. Ruoff, The chemistry of graphene oxide, *Chem. Soc. Rev.*, 2010, **39**, 228–240.
23 A. M. Dimiev and J. M. Tour, Mechanism of graphene oxide formation, *ACS Nano*, 2014, **8**, 3060–3068.
24 B. C. Brodie, XIII. On the atomic weight of graphite, *Philos. Trans. R. Soc. London*, 1859, **149**, 249–259.
25 A. Lerf, H. He, M. Forster and J. Klinowski, Structure of graphite oxide revisited, *J. Phys. Chem. B*, 1998, **102**, 4477–4482.
26 W. Gao, *Graphene oxide: Reduction recipes, spectroscopy, and applications*, Springer International Publishing, 2015, pp. 61–95.
27 D. R. Dreyer, A. D. Todd and C. W. Bielawski, Harnessing the chemistry of graphene oxide, *Chem. Soc. Rev.*, 2014, **43**, 5288–5301.
28 S. Stankovich, D. A. Dikin, R. D. Piner, K. A. Kohlhaas, A. Kleinhammes, Y. Jia, Y. Wu, S. T. Nguyen and R. S. Ruoff, Synthesis of graphene-based nanosheets *via* chemical reduction of exfoliated graphite oxide, *Carbon*, 2007, **45**, 1558–1565.
29 S. Stankovich, D. A. Dikin, G. H. B. Dommett, K. M. Kohlhaas, E. J. Zimney, E. A. Stach, R. D. Piner, S. T. Nguyen and R. S. Ruoff, Graphene-based composite materials, *Nature*, 2006, **442**, 282–286.
30 H.-J. Shin, K. K. Kim, A. Benayad, S.-M. Yoon, H. K. Park, I.-S. Jung, M. H. Jin, H.-K. Jeong, J. M. Kim, J.-Y. Choi and Y. H. Lee, Efficient reduction of graphite oxide by sodium borohydride and its effect on electrical conductance, *Adv. Funct. Mater.*, 2009, **19**, 1987–1992.
31 I. K. Moon, J. Lee, R. S. Ruoff and H. Lee, Reduced graphene oxide by chemical graphitization, *Nat. Commun.*, 2010, **1**, 73.
32 S. Pei and H.-M. Cheng, The reduction of graphene oxide, *Carbon*, 2012, **50**, 3210–3228.

33 C. K. Chua and M. Pumera, Chemical reduction of graphene oxide: A synthetic chemistry viewpoint, *Chem. Soc. Rev.*, 2014, **43**, 291–312.
34 D. Yu, Y. Yang, M. Durstock, J.-B. Baek and L. Dai, Soluble P3HT-grafted graphene for efficient bilayer-heterojunction photovoltaic devices, *ACS Nano*, 2010, **4**, 5633–5640.
35 X.-Z. Tang, W. Li, Z.-Z. Yu, M. A. Rafiee, J. Rafiee, F. Yavari and N. Koratkar, Enhanced thermal stability in graphene oxide covalently functionalized with 2-amino-4,6-didodecylamino-1,3,5-triazine, *Carbon*, 2011, **49**, 1258–1265.
36 Y. Xu, Z. Liu, X. Zhang, Y. Wang, J. Tian, Y. Huang, Y. Ma, X. Zhang and Y. Chen, A graphene hybrid material covalently functionalized with porphyrin: Synthesis and optical limiting property, *Adv. Mater.*, 2009, **21**, 1275–1279.
37 H. Bao, Y. Pan, Y. Ping, N. G. Sahoo, T. Wu, L. Li, J. Li and L. H. Gan, Chitosan-functionalized graphene oxide as a nanocarrier for drug and gene delivery, *Small*, 2011, **7**, 1569–1578.
38 J. T. Robinson, S. M. Tabakman, Y. Liang, H. Wang, H. Sanchez Casalongue, D. Vinh and H. Dai, Ultrasmall reduced graphene oxide with high near-infrared absorbance for photothermal therapy, *J. Am. Chem. Soc.*, 2011, **133**, 6825–6831.
39 M. Park, K. Song, T. Lee, J. Cha, I. Lyo and B.-S. Kim, Tailoring graphene nanosheets for highly improved dispersion stability and quantitative assessment in non-aqueous solvent, *ACS Appl. Mater. Interfaces*, 2016, **8**, 21595–21602.
40 T. T. Nguyen, P. Bandyopadhyay, X. Li, N. H. Kim and J. H. Lee, Effects of grafting methods for functionalization of graphene oxide by dodecylamine on the physical properties of its polyurethane nanocomposites, *J. Membr. Sci.*, 2017, **540**, 108–119.
41 M. Park, T. Lee and B.-S. Kim, Covalent functionalization based heteroatom doped graphene nanosheet as a metal-free electrocatalyst for oxygen reduction reaction, *Nanoscale*, 2013, **5**, 12255–12260.
42 H. Hwang, P. Joo, M. S. Kang, G. Ahn, J. T. Han, B.-S. Kim and J. H. Cho, Highly tunable charge transport in layer-by-layer assembled graphene transistors, *ACS Nano*, 2012, **6**, 2432–2440.
43 B. Park, W. Lee, E. Lee, S. H. Min and B.-S. Kim, Highly tunable interfacial adhesion of glass fiber by hybrid multilayers of graphene oxide and aramid nanofiber, *ACS Appl. Mater. Interfaces*, 2015, **7**, 3329–3334.
44 Y. Choi, D. Jeon, Y. Choi, D. Kim, N. Kim, M. Gu, S. Bae, T. Lee, H.-W. Lee, B.-S. Kim and J. Ryu, Interface engineering of hematite with nacre-like catalytic multilayers for solar water oxidation, *ACS Nano*, 2019, **13**, 467–475.
45 E. Ahn, T. Lee, M. Gu, M. Park, S. H. Min and B.-S. Kim, Layer-by-layer assembly for graphene-based multilayer nanocomposites: The field manual, *Chem. Mater.*, 2017, **29**, 69–79.
46 Y. Lin, J. Jin and M. Song, Preparation and characterisation of covalent polymer functionalized graphene oxide, *J. Mater. Chem.*, 2011, **21**, 3455–3461.
47 K. S. Kim, Y. Zhao, H. Jang, S. Y. Lee, J. M. Kim, K. S. Kim, J.-H. Ahn, P. Kim, J.-Y. Choi and B. H. Hong, Large-scale pattern growth of graphene films for stretchable transparent electrodes, *Nature*, 2009, **457**, 706–710.
48 X.-D. Zhuang, Y. Chen, G. Liu, P.-P. Li, C.-X. Zhu, E.-T. Kang, K.-G. Noeh, B. Zhang, J.-H. Zhu and Y.-X. Li, Conjugated-polymer-functionalized graphene oxide: Synthesis and nonvolatile rewritable memory effect, *Adv. Mater.*, 2010, **22**, 1731–1735.
49 B. T. McGrail, B. J. Rodier and E. Pentzer, Rapid functionalization of graphene oxide in water, *Chem. Mater.*, 2014, **26**, 5806–5811.
50 X. Ou, L. Jiang, P. Chen, M. Zhu, W. Hu, M. Liu, J. Zhu and H. Ju, Highly stable graphene-based multilayer films immobilized via covalent bonds and their applications in organic field-effect transistors, *Adv. Funct. Mater.*, 2013, **23**, 2422–2435.
51 H. Yao, L. Jin, H.-J. Sue, Y. Sumi and R. Nishimura, Facile decoration of Au nanoparticles on reduced graphene oxide surfaces *via* a one-step chemical functionalization approach, *J. Mater. Chem. A*, 2013, **1**, 10783–10789.
52 J. Ou, Y. Wang, J. Wang, S. Liu, Z. Li and S. Yang, Self-assembly of octadecyltrichlorosilane on graphene oxide and the tribological performances of the resultant film, *J. Phys. Chem. C*, 2011, **115**, 10080–10086.
53 W. R. Collins, W. Lewandowski, E. Schmois, J. Walish and T. M. Swager, Claisen rearrangement of graphite oxide: A route to covalently functionalized graphenes, *Angew. Chem., Int. Ed.*, 2011, **50**, 8848–8852.
54 W. R. Collins, E. Schmois and T. M. Swager, Graphene oxide as an electrophile for carbon nucleophiles, *Chem. Commun.*, 2011, **47**, 8790–8792.
55 L. Dai, Functionalization of graphene for efficient energy conversion and storage, *Acc. Chem. Res.*, 2013, **46**, 31–42.
56 C. E. Hamilton, J. R. Lomeda, Z. Sun, J. M. Tour and A. R. Barron, High-yield organic dispersions of unfunctionalized graphene, *Nano Lett.*, 2009, **9**, 3460–3462.
57 J. R. Lomeda, C. D. Doyle, D. V. Kosynkin, W.-F. Hwang and J. M. Tour, Diazonium functionalization of surfactant-wrapped chemically converted graphene sheets, *J. Am. Chem. Soc.*, 2008, **130**, 16201–16206.
58 J. Ji, G. Zhang, H. Chen, S. Wang, G. Zhang, F. Zhang and X. Fan, Sulfonated graphene as water-tolerant solid acid catalyst, *Chem. Sci.*, 2011, **2**, 484–487.
59 Z. Jin, T. P. McNicholas, C.-J. Shih, Q. H. Wang, G. L. C. Paulus, A. J. Hilmer, S. Shimizu and M. S. Strano, Click chemistry on solution-dispersed graphene and monolayer CVD graphene, *Chem. Mater.*, 2011, **23**, 3362–3370.
60 N. D. Luong, L. H. Sinh, L.-S. Johansson, J. Campell and J. Seppälä, Functional graphene by thiol-ene click chemistry, *Chem. – Eur. J.*, 2015, **21**, 3183–3186.
61 S. Sun, Y. Cao, J. Feng and P. Wu, Click chemistry as a route for the immobilization of well-defined polystyrene onto graphene sheets, *J. Mater. Chem.*, 2010, **20**, 5605–5607.

62 Y. Cao, Z. Lai, J. Feng and P. Wu, Graphene oxide sheets covalently functionalized with block copolymers via click chemistry as reinforcing fillers, *J. Mater. Chem.*, 2011, **21**, 9271–9278.
63 F. Meng, H. Ishida and X. Liu, Introduction of benzoxazine onto the graphene oxide surface by click chemistry and the properties of graphene oxide reinforced polybenzoxazine nanohybrids, *RSC Adv.*, 2014, **4**, 9471–9475.
64 G. Xu, P. Xu, D. Shi and M. Chen, Modification of graphene oxide by a facile coprecipitation method and click chemistry for use as a drug carrier, *RSC Adv.*, 2014, **4**, 28807–28813.
65 Y. Oz, A. Barras, R. Sanyal, R. Boukherroub, S. Szunerits and A. Sanyal, Functionalization of reduced graphene oxide *via* thiol–maleimide "click" chemistry: Facile fabrication of targeted drug delivery vehicles, *ACS Appl. Mater. Interfaces*, 2017, **9**, 34194–34203.
66 J. I. Paredes, S. Villar-Rodil, A. Martínez-Alonso and J. M. D. Tascón, Graphene oxide dispersions in organic solvents, *Langmuir*, 2008, **24**, 10560–10564.
67 Y. Si and E. T. Samulski, Synthesis of water soluble graphene, *Nano Lett.*, 2008, **8**, 1679–1682.
68 Y. Liu, D. Yu, C. Zeng, Z. Miao and L. Dai, Biocompatible graphene oxide-based glucose biosensors, *Langmuir*, 2010, **26**, 6158–6160.
69 F. Liu, J. Y. Choi and T. S. Seo, Graphene oxide arrays for detecting specific DNA hybridization by fluorescence resonance energy transfer, *Biosens. Bioelectron.*, 2010, **25**, 2361–2365.
70 C.-H. Lu, H.-H. Yang, C.-L. Zhu, X. Chen and G.-N. Chen, A graphene platform for sensing biomolecules, *Angew. Chem., Int. Ed.*, 2009, **48**, 4785–4787.
71 A. K. Yagati, J. Min and S. Cho, Electrosynthesis of ERGO-NP nanocomposite films for bioelectrocatalysis of horseradish peroxidase towards H_2O_2, *J. Electrochem. Soc.*, 2014, **161**, G133–G140.
72 S. Stankovich, R. D. Piner, S. T. Nguyen and R. S. Ruoff, Synthesis and exfoliation of isocyanate-treated graphene oxide nanoplatelets, *Carbon*, 2006, **44**, 3342–3347.
73 X. Yang, L. Ma, S. Wang, Y. Li, Y. Tu and X. Zhu, "Clicking" graphite oxide sheets with well-defined polystyrenes: A new strategy to control the layer thickness, *Polymer*, 2011, **52**, 3046–3052.
74 W. Zhang, S. Wang, J. Ji, Y. Li, G. Zhang, F. Zhang and X. Fan, Primary and tertiary amines bifunctional graphene oxide for cooperative catalysis, *Nanoscale*, 2013, **5**, 6030–6033.
75 N. Porahmad and R. Baharfar, Graphene oxide covalently functionalized with an organic superbase as highly efficient and durable nanocatalyst for green Michael addition reaction, *Res. Chem. Intermed.*, 2018, **44**, 305–323.
76 Y. Hou, D. Wang, X.-M. Zhang, H. Zhao, J.-W. Zha and Z.-M. Dang, Positive piezoresistive behavior of electrically conductive alkyl-functionalized graphene/polydimethylsilicone nanocomposites, *J. Mater. Chem. C*, 2013, **1**, 515–521.
77 N. A. Ismail, N. W. Mohd Zulkifli, Z. Z. Chowdhury and M. R. Johan, Grafting of straight alkyl chain improved the hydrophobicity and tribological performance of graphene oxide in oil as lubricant, *J. Mol. Liq.*, 2020, **319**, 114276.
78 S. Kumari, O. P. Sharma, R. Gusain, H. P. Mungse, A. Kukrety, N. Kumar, H. Sugimura and O. P. Khatri, Alkyl-chain-grafted hexagonal boron nitride nanoplatelets as oil-dispersible additives for friction and wear reduction, *ACS Appl. Mater. Interfaces*, 2015, **7**, 3708–3716.
79 R. Tan, C. Li, J. Luo, Y. Kong, W. Zheng and D. Yin, An effective heterogeneous L-proline catalyst for the direct asymmetric aldol reaction using graphene oxide as support, *J. Catal.*, 2013, **298**, 138–147.
80 W.-S. Ma, J. Li and X.-S. Zhao, Improving the thermal and mechanical properties of silicone polymer by incorporating functionalized graphene oxide, *J. Mater. Sci.*, 2013, **48**, 5287–5294.
81 S. S. Rawat, A. P. Harsha, O. P. Khatri and R. Wäsche, Pristine, reduced, and alkylated graphene oxide as additives to paraffin grease for enhancement of tribological properties, *J. Tribol.*, 2021, **143**, 021903.
82 B. Yu, K. Wang, Y. Hu, F. Nan, J. Pu, H. Zhao and P. Ju, Tribological properties of synthetic base oil containing polyhedral oligomeric silsesquioxane grafted graphene oxide, *RSC Adv.*, 2018, **8**, 23606–23614.
83 D. Berman, A. Erdemir and A. V. Sumant, Graphene: A new emerging lubricant, *Mater. Today*, 2014, **17**, 31–42.
84 M. D. Stoller, S. Park, Y. Zhu, J. An and R. S. Ruoff, Graphene-based ultracapacitors, *Nano Lett.*, 2008, **8**, 3498–3502.
85 C. Lee, X. Wei, J. W. Kysar and J. Hone, Measurement of the elastic properties and intrinsic strength of monolayer graphene, *Science*, 2008, **321**, 385–388.
86 A. A. Balandin, S. Ghosh, W. Bao, I. Calizo, D. Teweldebrhan, F. Miao and C. N. Lau, Superior thermal conductivity of single-layer graphene, *Nano Lett.*, 2008, **8**, 902–907.
87 H. P. Mungse and O. P. Khatri, Chemically functionalized reduced graphene oxide as a novel material for reduction of friction and wear, *J. Phys. Chem. C*, 2014, **118**, 14394–14402.
88 S. Choudhary, H. P. Mungse and O. P. Khatri, Dispersion of alkylated graphene in organic solvents and its potential for lubrication applications, *J. Mater. Chem.*, 2012, **22**, 21032–21039.
89 H. P. Mungse, N. Kumar and O. P. Khatri, Synthesis, dispersion and lubrication potential of basal plane functionalized alkylated graphene nanosheets, *RSC Adv.*, 2015, **5**, 25565–25571.
90 Z.-L. Cheng, W. Li, P.-R. Wu and Z. Liu, A strategy for preparing modified graphene oxide with good dispersibility and transparency in oil, *Ind. Eng. Chem. Res.*, 2017, **56**, 5527–5534.
91 N. A. Ismail and S. Bagheri, Highly oil-dispersed functionalized reduced graphene oxide nanosheets as lube oil friction modifier, *Mater. Sci. Eng., B*, 2017, **222**, 34–42.
92 T. S. Sreeprasad and V. Berry, How do the electrical properties of graphene change with its functionalization?, *Small*, 2013, **9**, 341–350.

93 S. Alipoori, M. M. Torkzadeh, M. H. M. Moghadam, S. Mazinani, S. H. Aboutalebi and F. Sharif, Graphene oxide: An effective ionic conductivity promoter for phosphoric acid-doped poly(vinyl alcohol) gel electrolytes, *Polymer*, 2019, **184**, 121908.

94 P. Dai, Z.-H. Mo, R.-W. Xu, S. Zhang, X. Lin, W.-F. Lin and Y.-X. Wu, Development of a cross-linked quaternized poly(styrene-*b*-isobutylene-*b*-styrene)/graphene oxide composite anion exchange membrane for direct alkaline methanol fuel cell application, *RSC Adv.*, 2016, **6**, 52122–52130.

95 L. Liu, C. Tong, Y. He, Y. Zhao and C. Lü, Enhanced properties of quaternized graphenes reinforced polysulfone based composite anion exchange membranes for alkaline fuel cell, *J. Membr. Sci.*, 2015, **487**, 99–108.

96 C. Long, C. Lu, Y. Li, Z. Wang and H. Zhu, N-spirocyclic ammonium-functionalized graphene oxide-based anion exchange membrane for fuel cells, *Int. J. Hydrogen Energy*, 2020, **45**, 19778–19790.

97 S. Thakur and N. Karak, Alternative methods and nature-based reagents for the reduction of graphene oxide: A review, *Carbon*, 2015, **94**, 224–242.

98 R. Li, Y. Yang, D. Wu, K. Li, Y. Qin, Y. Tao and Y. Kong, Covalent functionalization of reduced graphene oxide aerogels with polyaniline for high performance supercapacitors, *Chem. Commun.*, 2019, **55**, 1738–1741.

99 P. Tang, L. Han, P. Li, Z. Jia, K. Wang, H. Zhang, H. Tan, T. Guo and X. Lu, Mussel-inspired electroactive and antioxidative scaffolds with incorporation of polydopamine-reduced graphene oxide for enhancing skin wound healing, *ACS Appl. Mater. Interfaces*, 2019, **11**, 7703–7714.

100 R. D. Rodriguez, A. Khalelov, P. S. Postnikov, A. Lipovka, E. Dorozhko, I. Amin, G. V. Murastov, J.-J. Chen, W. Sheng, M. E. Trusova, M. M. Chehimi and E. Sheremet, Beyond graphene oxide: Laser engineering functionalized graphene for flexible electronics, *Mater. Horiz.*, 2020, **7**, 1030–1041.

101 J.-S. Lee, T. Lee, H.-K. Song, J. Cho and B.-S. Kim, Ionic liquid modified graphene nanosheets anchoring manganese oxide nanoparticles as efficient electrocatalysts for Zn–air batteries, *Energy Environ. Sci.*, 2011, **4**, 4148–4154.

102 E. Kowsari and M. R. Chirani, High efficiency dye-sensitized solar cells with tetra alkyl ammonium cation-based ionic liquid functionalized graphene oxide as a novel additive in nanocomposite electrolyte, *Carbon*, 2017, **118**, 384–392.

103 J. Li, H. Wu, L. Cao, X. He, B. Shi, Y. Li, M. Xu and Z. Jiang, Enhanced proton conductivity of sulfonated polysulfone membranes under low humidity *via* the incorporation of multifunctional graphene oxide, *ACS Appl. Nano Mater.*, 2019, **2**, 4734–4743.

104 E. K. Jeon, E. Seo, E. Lee, W. Lee, M.-K. Um and B.-S. Kim, Mussel-inspired green synthesis of silver nanoparticles on graphene oxide nanosheets for enhanced catalytic applications, *Chem. Commun.*, 2013, **49**, 3392–3394.

105 D. R. Dreyer and C. W. Bielawski, Carbocatalysis: Heterogeneous carbons finding utility in synthetic chemistry, *Chem. Sci.*, 2011, **2**, 1233–1240.

106 D. R. Dreyer, H.-P. Jia and C. W. Bielawski, Graphene oxide: A convenient carbocatalyst for facilitating oxidation and hydration reactions, *Angew. Chem., Int. Ed.*, 2010, **49**, 6813–6816.

107 C. Su, M. Acik, K. Takai, J. Lu, S.-J. Hao, Y. Zheng, P. Wu, Q. Bao, T. Enoki, Y. J. Chabal and K. Ping Loh, Probing the catalytic activity of porous graphene oxide and the origin of this behaviour, *Nat. Commun.*, 2012, **3**, 1298.

108 F. Zhang, H. Jiang, X. Li, X. Wu and H. Li, Amine-functionalized GO as an active and reusable acid–base bifunctional catalyst for one-pot cascade reactions, *ACS Catal.*, 2014, **4**, 394–401.

109 S. Navalon, A. Dhakshinamoorthy, M. Alvaro and H. Garcia, Carbocatalysis by graphene-based materials, *Chem. Rev.*, 2014, **114**, 6179–6212.

110 A. Corma, S. Iborra and A. Velty, Chemical routes for the transformation of biomass into chemicals, *Chem. Rev.*, 2007, **107**, 2411–2502.

111 E. Lam, J. H. Chong, E. Majid, Y. Liu, S. Hrapovic, A. C. W. Leung and J. H. T. Luong, Carbocatalytic dehydration of xylose to furfural in water, *Carbon*, 2012, **50**, 1033–1043.

112 M. M. Antunes, P. A. Russo, P. V. Wiper, J. M. Veiga, M. Pillinger, L. Mafra, D. V. Evtuguin, N. Pinna and A. A. Valente, Sulfonated graphene oxide as effective catalyst for conversion of 5-(hydroxymethyl)-2-furfural into biofuels, *ChemSusChem*, 2014, **7**, 804–812.

113 S. Verma, H. P. Mungse, N. Kumar, S. Choudhary, S. L. Jain, B. Sain and O. P. Khatri, Graphene oxide: An efficient and reusable carbocatalyst for aza-Michael addition of amines to activated alkenes, *Chem. Commun.*, 2011, **47**, 12673–12675.

114 M. R. Acocella, M. Mauro and G. Guerra, Regio- and enantioselective Friedel–Crafts reactions of indoles to epoxides catalyzed by graphene oxide: A green approach, *ChemSusChem*, 2014, **7**, 3279–3283.

115 A. Dhakshinamoorthy, M. Alvaro, P. Concepción, V. Fornés and H. Garcia, Graphene oxide as an acid catalyst for the room temperature ring opening of epoxides, *Chem. Commun.*, 2012, **48**, 5443–5445.

116 L. Wang, D. Wang, S. Zhang and H. Tian, Synthesis and characterization of sulfonated graphene as a highly active solid acid catalyst for the ester-exchange reaction, *Catal. Sci. Technol.*, 2013, **3**, 1194–1197.

117 K. Li, J. Chen, Y. Yan, Y. Min, H. Li, F. Xi, J. Liu and P. Chen, Quasi-homogeneous carbocatalysis for one-pot selective conversion of carbohydrates to 5-hydroxymethylfurfural using sulfonated graphene quantum dots, *Carbon*, 2018, **136**, 224–233.

118 A. Dhakshinamoorthy, M. Alvaro, M. Puche, V. Fornes and H. Garcia, Graphene oxide as catalyst for the acetalization of aldehydes at room temperature, *ChemCatChem*, 2012, **4**, 2026–2030.

119 Y. Li, Q. Zhao, J. Ji, G. Zhang, F. Zhang and X. Fan, Cooperative catalysis by acid–base bifunctional graphene, *RSC Adv.*, 2013, **3**, 13655–13658.

120 P. Kumar, B. Sain and S. L. Jain, Photocatalytic reduction of carbon dioxide to methanol using a ruthenium trinuclear polyazine complex immobilized on graphene oxide under visible light irradiation, *J. Mater. Chem. A*, 2014, **2**, 11246–11253.

121 Y.-H. Yao, J. Li, H. Zhang, H.-L. Tang, L. Fang, G.-D. Niu, X.-J. Sun and F.-M. Zhang, Facile synthesis of a covalently connected RGO–COF hybrid material by *in situ* reaction for enhanced visible-light induced photocatalytic H_2 evolution, *J. Mater. Chem. A*, 2020, **8**, 8949–8956.

122 Z. Fang, A. Ito, A. C. Stuart, H. Luo, Z. Chen, K. Vinodgopal, W. You, T. J. Meyer and D. K. Taylor, Soluble reduced graphene oxide sheets grafted with polypyridylruthenium-derivatized polystyrene brushes as light harvesting antenna for photovoltaic applications, *ACS Nano*, 2013, **7**, 7992–8002.

123 R. Vinoth, S. G. Babu, V. Bharti, V. Gupta, M. Navaneethan, S. V. Bhat, C. Muthamizhchelvan, P. C. Ramamurthy, C. Sharma, D. K. Aswal, Y. Hayakawa and B. Neppolian, Ruthenium based metallopolymer grafted reduced graphene oxide as a new hybrid solar light harvester in polymer solar cells, *Sci. Rep.*, 2017, **7**, 43133.

124 P. Kumar, A. Kumar, B. Sreedhar, B. Sain, S. S. Ray and S. L. Jain, Cobalt phthalocyanine immobilized on graphene oxide: An efficient visible-active catalyst for the photoreduction of carbon dioxide, *Chem. – Eur. J.*, 2014, **20**, 6154–6161.

125 P. Kumar, A. Bansiwal, N. Labhsetwar and S. L. Jai, Visible light assisted photocatalytic reduction of CO_2 using a graphene oxide supported heteroleptic ruthenium complex, *Green Chem.*, 2015, **17**, 1605–1609.

126 C.-X. Tian, S.-C. Cui, X.-Y. Liu and J.-G. Liu, A hybrid composite of rhenium complexes covalently grafted on reduced graphene oxide/hydrogenated TiO_2 as an efficient catalyst for CO_2 reduction under visible light, *Res. Chem. Intermed.*, 2020, **46**, 1–13.

127 V. S. Sapner, B. B. Mulik, R. V. Digraskar, S. S. Narwade and B. R. Sathe, Enhanced oxygen evolution reaction on amine functionalized graphene oxide in alkaline medium, *RSC Adv.*, 2019, **9**, 6444–6451.

128 L. Dai, Y. Xue, L. Qu, H.-J. Choi and J.-B. Baek, Metal-free catalysts for oxygen reduction reaction, *Chem. Rev.*, 2015, **115**, 4823–4892.

129 X. Ren, Y. Wang, A. Liu, Z. Zhang, Q. Lv and B. Liu, Current progress and performance improvement of Pt/C catalysts for fuel cells, *J. Mater. Chem. A*, 2020, **8**, 24284–24306.

130 Z. Zhao, C. Chen, Z. Liu, J. Huang, M. Wu, H. Liu, Y. Li and Y. Huang, Pt-Based nanocrystal for electrocatalytic oxygen reduction, *Adv. Mater.*, 2019, **31**, 1808115.

131 X. Liu and L. Dai, Carbon-based metal-free catalysts, *Nat. Rev. Mater.*, 2016, **1**, 16064.

132 J. Lai, A. Nsabimana, R. Luque and G. Xu, 3D porous carbonaceous electrodes for electrocatalytic applications, *Joule*, 2018, **2**, 76–93.

133 F. Li, X. Jiang, J. Zhao and S. Zhang, Graphene oxide: A promising nanomaterial for energy and environmental applications, *Nano Energy*, 2015, **16**, 488–515.

134 C. K. Chua and M. Pumera, Monothiolation and reduction of graphene oxide via one-pot synthesis: Hybrid catalyst for oxygen reduction, *ACS Nano*, 2015, **9**, 4193–4199.

135 J. Park and M. Yan, Covalent functionalization of graphene with reactive intermediates, *Acc. Chem. Res.*, 2013, **46**, 181–189.

136 Y. Jin, Y. Zheng, S. G. Podkolzin and W. Lee, Band gap of reduced graphene oxide tuned by controlling functional groups, *J. Mater. Chem. C*, 2020, **8**, 4885–4894.

137 A. Kaplan, Z. Yuan, J. D. Benck, A. Govind Rajan, X. S. Chu, Q. H. Wang and M. S. Strano, Current and future directions in electron transfer chemistry of graphene, *Chem. Soc. Rev.*, 2017, **46**, 4530–4571.

138 A. Navaee and A. Salimi, Efficient amine functionalization of graphene oxide through the bucherer reaction: An extraordinary metal-free electrocatalyst for the oxygen reduction reaction, *RSC Adv.*, 2015, **5**, 59874–59880.

139 V. S. Sapner, P. P. Chavan and B. R. Sathe, L-Lysine-functionalized reduced graphene oxide as a highly efficient electrocatalyst for enhanced oxygen evolution reaction, *ACS Sustainable Chem. Eng.*, 2020, **8**, 5524–5533.

140 M. S. Ahmed and Y.-B. Kim, 3D graphene preparation via covalent amide functionalization for efficient metal-free electrocatalysis in oxygen reduction, *Sci. Rep.*, 2017, **7**, 43279.

141 J. Yuan, W.-Y. Zhi, L. Liu, M.-P. Yang, H. Wang and J.-X. Lu, Electrochemical reduction of CO_2 at metal-free N-functionalized graphene oxide electrodes, *Electrochim. Acta*, 2018, **282**, 694–701.

142 C. Hu and L. Dai, Doping of carbon materials for metal-free electrocatalysis, *Adv. Mater.*, 2019, **31**, 1804672.

143 J. Duan, S. Chen, M. Jaroniec and S. Z. Qiao, Heteroatom-doped graphene-based materials for energy-relevant electrocatalytic processes, *ACS Catal.*, 2015, **5**, 5207–5234.

144 Y. Zheng, Y. Jiao, Y. Zhu, L. H. Li, Y. Han, Y. Chen, A. Du, M. Jaroniec and S. Z. Qiao, Hydrogen evolution by a metal-free electrocatalyst, *Nat. Commun.*, 2014, **5**, 3783.

145 R. Paul, Q. Dai, C. Hu and L. Dai, Ten years of carbon-based metal-free electrocatalysts, *Carbon Energy*, 2019, **1**, 19–31.

146 S. Kaushal, M. Kaur, N. Kaur, V. Kumari and P. P. Singh, Heteroatom-doped graphene as sensing materials: A mini review, *RSC Adv.*, 2020, **10**, 28608–28629.

147 W. Zheng, Y. Zhang, K. Niu, T. Liu, K. Bustillo, P. Ercius, D. Nordlund, J. Wu, H. Zheng and X. Du, Selective nitrogen doping of graphene oxide by laser irradiation for enhanced hydrogen evolution activity, *Chem. Commun.*, 2018, **54**, 13726–13729.

148 S. Agnoli and M. Favaro, Doping graphene with boron: A review of synthesis methods, physicochemical characterization, and emerging applications, *J. Mater. Chem. A*, 2016, **4**, 5002–5025.

149 J. Zhang and L. Dai, Heteroatom-doped graphitic carbon catalysts for efficient electrocatalysis of oxygen reduction reaction, *ACS Catal.*, 2015, **5**, 7244–7253.

150 X. Yu, P. Han, Z. Wei, L. Huang, Z. Gu, S. Peng, J. Ma and G. Zheng, Boron-doped graphene for electrocatalytic N_2 reduction, *Joule*, 2018, **2**, 1610–1622.

151 R. Li, Z. Wei and X. Gou, Nitrogen and phosphorus dual-doped graphene/carbon nanosheets as bifunctional electrocatalysts for oxygen reduction and evolution, *ACS Catal.*, 2015, **5**, 4133–4142.

152 A. Wang, C. Li, J. Zhang, X. Chen, L. Cheng and W. Zhu, Graphene-oxide-supported covalent organic polymers based on zinc phthalocyanine for efficient optical limiting and hydrogen evolution, *J. Colloid Interface Sci.*, 2019, **556**, 159–171.

153 A. A. Ensafi, M. Jafari-Asl and B. Rezaei, Pyridine-functionalized graphene oxide, an efficient metal free electrocatalyst for oxygen reduction reaction, *Electrochim. Acta*, 2016, **194**, 95–103.

154 S. Song, Y. Xue, L. Feng, H. Elbatal, P. Wang, C. N. Moorefield, G. R. Newkome and L. Dai, Reversible self-assembly of terpyridine-functionalized graphene oxide for energy conversion, *Angew. Chem., Int. Ed.*, 2014, **53**, 1415–1419.

155 M. Jahan, Q. Bao and K. P. Loh, Electrocatalytically active graphene–porphyrin MOF composite for oxygen reduction reaction, *J. Am. Chem. Soc.*, 2012, **134**, 6707–6713.

156 K. Qu, Y. Zheng, S. Dai and S. Z. Qiao, Graphene oxide-polydopamine derived N,S-codoped carbon nanosheets as superior bifunctional electrocatalysts for oxygen reduction and evolution, *Nano Energy*, 2016, **19**, 373–381.

157 Y. Ito, W. Cong, T. Fujita, Z. Tang and M. Chen, High catalytic activity of nitrogen and sulfur co-doped nanoporous graphene in the hydrogen evolution reaction, *Angew. Chem., Int. Ed.*, 2015, **54**, 2131–2136.

158 L. Jiang, L. Qiu, T. Cen, Y.-Y. Liu, X. Peng, Z. Ye and D. Yuan, Controllable Co@N-doped graphene anchored onto the NRGO toward electrocatalytic hydrogen evolution at all pH values, *Chem. Commun.*, 2020, **56**, 567–570.

159 J. H. Dumont, U. Martinez, K. Artyushkova, G. M. Purdy, A. M. Dattelbaum, P. Zelenay, A. Mohite, P. Atanassov and G. Gupta, Nitrogen-doped graphene oxide electrocatalysts for the oxygen reduction reaction, *ACS Appl. Nano Mater.*, 2019, **2**, 1675–1682.

160 P. Su, K. Iwase, S. Nakanishi, K. Hashimoto and K. Kamiya, Nickel–nitrogen-modified graphene: An efficient electrocatalyst for the reduction of carbon dioxide to carbon monoxide, *Small*, 2016, **12**, 6083–6089.

161 Z. Lin, G. H. Waller, Y. Liu, M. Liu and C.-p. Wong, 3D nitrogen-doped graphene prepared by pyrolysis of graphene oxide with polypyrrole for electrocatalysis of oxygen reduction reaction, *Nano Energy*, 2013, **2**, 241–248.

162 J. Cai, P. Ruffieux, R. Jaafar, M. Bieri, T. Braun, S. Blankenburg, M. Muoth, A. P. Seitsonen, M. Saleh, X. Feng, K. Müllen and R. Fasel, Atomically precise bottom-up fabrication of graphene nanoribbons, *Nature*, 2010, **466**, 470–473.

163 J. Chen, Y. Li, L. Huang, N. Jia, C. Li and G. Shi, Size fractionation of graphene oxide sheets via filtration through track-etched membranes, *Adv. Mater.*, 2015, **27**, 3654–3660.

164 B. Zhang, L. Fan, H. Zhong, Y. Liu and S. Chen, Graphene nanoelectrodes: Fabrication and size-dependent electrochemistry, *J. Am. Chem. Soc.*, 2013, **135**, 10073–10080.

165 S. Li, F. Zhu, F. Meng, H. Li, L. Wang, J. Zhao, Q. Yue, J. Liu and J. Jia, Separation of graphene oxide by density gradient centrifugation and study on their morphology-dependent electrochemical properties, *J. Electroanal. Chem.*, 2013, **703**, 135–145.

